Classification of basins, with special reference to Proterozoic examples

P. A. ALLEN[1], P. G. ERIKSSON[2], F.F. ALKMIM[3], P.G. BETTS[4], O. CATUNEANU[5], R. MAZUMDER[6], Q. MENG[7], G.M. YOUNG[8]

[1]*Department of Earth Sciences and Engineering, South Kensington Campus, Imperial College, London SW7 2AZ, United Kingdom*

[2]*Department of Geology, University of Pretoria, Pretoria 0002, South Africa*

[3]*Departamento de Geologia, Escola de Minas, Universidade Federal de Ouro Preto, Morro do Cruzeiro, 35.400.000 Ouro Preto MG, Brazil*

[4]*School of Geosciences, Monash University, Wellington Road, Clayton, VIC 3800, Australia*

[5]*Department of Earth and Atmospheric Sciences, 1-26 Earth Sciences Building, University of Alberta, Edmonton, Alberta T6G 2E3, Canada*

[6] *School of Biological, Earth and Environmental Sciences, University of New South Wales, Kensington, Sydney, New South Wales 2052 Australia*

[7]*Institute of Geology and Geophysics, Chinese Academy of Sciences, Beijing 100029, China*

[8]*Department of Earth Sciences, Western University, London, Ontario N6A 5B7*

Abstract: Basin classification rests on a plate tectonic foundation, highlighting lithospheric substrate, proximity to plate margin and relative motion of the nearest plate boundary. Major mechanisms for regional subsidence and uplift are subdivided into isostatic, flexural and dynamic groups. Basin-forming mechanisms and basin types do not exhibit simple cause-and-effect relationships, but rather reflect a matrix-type relationship. Different basin types have different spans of existence, with generally shorter life spans related to more tectonically active settings. Many 'polyhistory' basins, composed of two or more megasequences, reflect a long evolution dominated by different basin-forming and basin-modifying mechanisms. The supercontinent cycle is marked by distinct sets of basin types, developed during successive phases of the cycle. Major classification schemes are reviewed briefly, before surveying the range of basin types represented in the Proterozoic of several key cratonic areas. Basins examined encompass almost the entire Neoarchaean – Neoproterozoic period. All these basins have a relatively long history of preservation, which can be tied to the essentially continental character of their basement rocks and concomitant enhanced "survivability". Their preservation thus underlines the longevity and inherent stability of the continental lithosphere. The distinction between basin occurrence over geological time and preferential preservation is important when viewing the geological record.

This paper serves as the more generalised of two introductory contributions to a volume on the Precambrian basins of India. The companion introductory paper (Meert and Pandit, this volume) is focused on the geological evolution of India and particularly the tectonic framework that accommodated evolution of the Indian Precambrian depositories. In contrast, the current article examines firstly the merits of basin classification schemes in order to provide a background for

the 17 regional papers on almost all important Precambrian basins of the Indian continent, which make up most of the volume. Secondly, this paper uses mainly Proterozoic basins from a set of specific cratons (Kaapvaal craton, Canadian shield, Brazilian shield, Australian continent and North China craton) to exemplify the intrinsic complexity of the natural record across the globe against the more generic basin classification schemes. In view of the comprehensive review of Indian Precambrian basins presented by Meert and Pandit (this volume) and the detailed basin studies making up the core of the book, it would have been superfluous for our paper to also include a review of the Aravalli-Bundelkand, Singhbhum, Bastar and Dharwar cratons of India. The final paper of the book (Miall et al., this volume) encompasses a summative comparison of the evolution of the Indian Precambrian basins with that of the global picture (which we here illustrate), thereby providing a unitary bridge between the two introductory papers and indeed uniting the entire volume in a concluding perspective.

Stephen J. Gould wrote in his book *Wonderful Life* (Gould, 1989, p.98) that

> 'Ideally, classifications are theories about the basis of natural order rather than dull catalogues compiled only to avoid chaos'

(quoted in Ingersoll & Busby, 1995, p. 2). In this sense, classification schemes for sedimentary basins should both reveal something of the underlying mechanisms for basin development and reflect the natural variability of the real world.

Historically, sedimentary basins have been classified in industry-based schemes using their large-scale architecture, including both cross-sectional geometry and planform shape, and hydrocarbon characteristics (Halbouty *et al*., 1970; Fischer, 1975; Huff, 1978; Klemme, 1980). For example, Klemme's (1980) scheme recognizes eight main types of basin based on their linearity, asymmetry, and cross-sectional geometry. Industry-based classifications have the common goal of categorizing a sedimentary basin and thereby gaining some predictive insights into its hydrocarbon potential. Although such classifications undoubtedly have their uses, particularly in predicting the presence of key elements of the petroleum play in a frontier basin, they have the effect of scrambling some of the essential differences and similarities between basins from the point of view of geodynamics.

Classification schemes of sedimentary basins based on plate tectonics emphasize the position of the basin in relation to the type of lithospheric substrate (continental, oceanic, transitional), the proximity of the basin to a plate margin (plate margin, plate interior), and the type of plate boundary nearest to the basin (divergent, convergent, transform) (Fig. 1). The evolution of a basin could then be explained by changing plate settings and interactions. Dickinson (1974), recognizing the rapid development in the understanding of global tectonics, proposed five major basin types on this basis:

Oceanic basins
Rifted continental margins
Arc-trench systems
Suture belts
Intracontinental basins

Reading (1982) and Miall (1990) added strike-slip or transform-related basins to this list.

The approach of Bally (1975) and Bally & Snelson (1980) was somewhat different. They differentiated three different families of sedimentary basins based on their location in relation to *megasutures*, which in this context can be defined to include all the products of orogenic and igneous activity associated with predominantly contractional deformation. The boundaries of megasutures are often associated with subduction, whether of slabs of oceanic lithosphere or of relatively buoyant continental lithosphere. They may also be the sites of important wrench tectonics along transform faults. Bally's three main families were (1) basins on rigid, stable lithosphere, (2) basins on rigid lithosphere outside contractional megasutures, called 'perisutural', and (3) basins situated within megasutures, termed 'episutural' (Fig. 2).

The linkage of basin development with plate tectonics was developed from Dickinson (1974) by a number of authors (Mitchell & Reading, 1986; Miall, 1990; Ingersoll & Busby, 1995; Einsele, 2000; Ingersoll, 2012), which led to a proliferation of basin types. Perhaps most conspicuous is the scheme proposed by Kingston *et al.* (1983a, b) which once again placed basins in their plate tectonic setting according to their lithospheric substrate, type of plate motion and proximity to plate margin, but categorized basins not only in relation to their basin-forming tectonics, but also in relation to the depositional sequences in the basin-fill and any basin-modifying tectonics (Fig. 1). A version of Kingston *et al.*'s (1983a) scheme modified by Mitchell & Reading (1986) is provided in Table 1. A flow chart ('decision tree') using and modifying Kingston *et al.*'s (1983a) scheme is given by Allen & Allen (2013, p.16) (Fig. 3).

Ingersoll & Busby (1995) and Ingersoll (2012) extended the classification of basins, making it more comprehensive to include 26 different basin types, but breaking down the system into 4 main categories based essentially on intraplate, divergent, convergent or transform kinematics (Table 2). Within these settings, Ingersoll (2012) suggested that there were numerous variants depending on sediment supply and geological inheritance.

Basin-forming mechanisms

A number of mechanisms may potentially be responsible for the subsidence of sedimentary basins, operating to different degree in different basin types (Fig. 4). These subsidence mechanisms (modified from Ingersoll & Busby (1995) and Ingersoll (2012)) can be summarized as:

1. crustal thinning, such as caused primarily by mechanical stretching or by surface erosion;
2. lithospheric thickening, such as caused by cooling following stretching, cooling due to sea-floor spreading away from an ocean ridge system, or by accretion of melts derived from the asthenosphere;
3. sedimentary and volcanic loading causing flexural compensation by long-wavelength bending;
4. tectonic (supracrustal) loading, such as caused by tectonic shortening in a zone of convergence, also causing flexural compensation;
5. subcrustal loading caused by subcrustal dense loads such as magmatic underplates or obducted mantle flakes;
6. long-wavelength buckling under a horizontal 'in-plane' stress;

7. mantle circulation primarily due to the subduction of cold lithospheric slabs;
8. crustal densification due to changing P-T conditions or intrusion of high-density melts.

Further details on these subsidence mechanisms can be found in Allen & Allen (2013). From the point of view of fundamental geodynamical processes, the major mechanisms for regional subsidence and uplift (*isostatic*, *flexural* and *dynamic*) can be summarized as follows (Fig. 5):

- *Isostatic* consequences of changes in crustal and lithospheric thickness; the thickness changes may be brought about purely thermally by *cooling* of mantle lithosphere, for example following a period of mechanical stretching. Thickness changes causing *thinning* may be caused by mechanical stretching, subaerial erosion of crust or at depth by removal (or delamination) of a deep lithospheric root. Mechanical *thickening* of crust and lithosphere, as in zones of continental convergence, generally causes isostatic uplift. Thickening of the lithosphere by cooling, however, causes subsidence.
- *Loading* and unloading at the surface and in the subsurface, including the far-field effects of in-plane stresses; *loading* of the lithosphere may take place on a small scale in the form of volcanoes or seamount chains, and on a large scale in the form of mountain belts, causing *flexure* and therefore subsidence. In-plane stresses may cause buckling of a rheologically layered lithosphere into a series of antiforms and synforms. The sediment infilling a basin also acts as a sedimentary load, amplifying the primary driving mechanism.
- *Dynamic* effects of asthenospheric flow, mantle convection and plumes; subsidence or uplift are caused by the buoyancy effects of changes in temperature in the mantle. Although some of temperature changes may result from chemical heterogeneity, most are generated by viscous flow, so the surface elevation changes may be termed *dynamic*.

For a given basin type, some or all of the mechanisms given above may have a major or minor role (Fig. 4). In addition, a given mechanism operates in more than one basin type. The classification scheme is therefore a matrix rather than a hierarchical 'flow chart' or 'decision tree' (Fig. 3).

Basins formed by stretching or thinning of the continental lithosphere fall within an evolutionary sequence known as the *rift-drift suite* (Kinsman, 1975; Veevers, 1981). The early stages of the sequence correspond to the development of intracontinental sags (cratonic basins) and continental rim basins, which generally lack clear evidence of brittle stretching, and continental rifts, which comprise clear extensional fault systems that may or may not be associated with topographic doming. Such rifts may evolve into oceanic spreading centres or may be aborted to form failed rifts. With seafloor creation and drifting of the continental edge away from the spreading centre, passive margin basins develop. The mechanisms of interest within this evolutionary sequence are therefore primarily the thermal and mechanical behaviour of the lithosphere under tension, the dynamic topography associated with hot underlying aesthenosphere, and the thermal contraction of the lithosphere following stretching.

Basins formed by flexure are mainly linked to plate convergence. Flexure of oceanic lithosphere as it approaches subduction zones is responsible for the formation of deep oceanic trenches. Flexure of the continental lithosphere in continental collision zones gives rise to foreland basins. Flexure of the lower or subducting plate generates *pro-foreland basins*, which are relatively short-lived and have convex-up subsidence profiles, whereas flexure of the upper or overriding plate generates *retro-foreland basins*, which are longer-lived and have slower, linear subsidence (Naylor & Sinclair, 2008). Where subduction zone roll-back takes place, as in

the Adriatic-Apennines region of Italy, the lower plate is flexed to produce a pro-foreland basin, but the retro-foreland region is extensional. Foreland basin pairs may also be associated with intracontinental mountain building where there is no subduction, as in the late Precambrian and Palaeozoic of central Australia. In some instances, a pro-foreland basin is present, but there is no retro-arc equivalent, as in Taiwan.

Processes within the mantle have an important role in basin development. Mantle flow structures, probably originating at the core–mantle boundary, impinge on the base of the lithosphere and spread out laterally over a length scale of 10^3 km. They are instrumental in continental splitting and the formation of new ocean basins, and have a major role in igneous underplating and isostatic regional uplift. Present-day *hotspots* over ascending limbs of mantle convection systems are characterized by topographic doming and commonly rifting. Basins located over downward limbs of convection systems, *cold-spot basins*, appear to be broad, gentle sags. The onset of subduction of cold oceanic slabs at ocean–continent boundaries causes far-field tilting of the continental plate towards its margin and therefore has a potentially major effect in forearc, intra-arc and retro-arc settings. In addition, supercontinental assemblies in the geological past have experienced very long wavelength topographic doming caused by elevated sub-lithospheric temperatures generated by an overlying insulating lid. Mantle flow instabilities associated with steps in the base of the lithosphere, or associated with the drip-like removal of gravitationally unstable mantle lithosphere, may also have important impacts on surface topography.

Time span and temporal occurrence of basin types

One of the first and most important tasks faced by the basin analyst is the break down of the long geological record of sedimentary basins into *megasequences*. Megasequences are the stratigraphic successions associated with a distinct phase of plate motion or which are deposited during the operation of a coherent set of formative mechanisms. Megasequences can be recognized by their bounding unconformities, which are always regional, commonly supra-regional, and possibly global, in extent. Some of these unconformities may be due to very widespread and prolonged uplift of the continental surface during continental amalgamation due to incubation of the underlying mantle (Grigné *et al*., 2007). Other megasequence boundaries may be due to changing patterns of dynamic topography caused by subduction around the continental margin (Burgess *et al*., 1997). These unconformities typically increase in erosional gap towards the continental interior, as in the ‘sequences’ of the US continental interior described long ago by Sloss (1963). Some megasequence boundaries are characterized by unconformities that are generated by uplift in a flexural forebulge region during the translation across the continental plate of an orogenic load system. Such unconformities have characteristic patterns of erosional gap and pass into conformities close to the orogenic load (Crampton & Allen, 1995). The result of the break down into megasequences is to illuminate the distinctly different phases that a sedimentary basin may have undergone. This is particularly important in long-lived basins.

Different basin types have a typical time span of existence (Ingersoll & Busby, 1995), after which they may be uplifted and eroded, locally inverted, or modified into another basin type to become *polyhistory* in nature. Each phase of existence will be recognized by a megasequence. Time spans of megasequences may range over 4 orders of magnitude (Woodcock, 2004).

Oceanic trench basins have the shortest life span (0.1-0.8 Myr) due to rapid subduction velocities and early incorporation into an accretionary wedge. Trench-slope, intra-arc, extensional back-arc and strike-slip basins also have relatively short life spans in the range 2-25 Myr, reflecting their tectonically active settings. Rift, forearc, back-arc and foreland basins have longer time spans in the range 4-125 Myr. The longest life spans (60-440 Myr) are found in intracratonic, passive margin and ocean basins, since they are situated in regions of low strain rate, experiencing prolonged thermal subsidence (Fig. 6).

Basin initiation and subsequent evolution can be related to the long-term cycle of plate aggregation into supercontinental assemblies, break-up and formation of new oceans, dispersal of continental fragments, subduction and collision (Anderson, 1982; Kerr, 1985; Nance *et al.*, 1988) (Fig. 6). This recurring signal in the geological record is marked by collisional orogenesis during continental assembly, and extrusive volcanism and rifting during break-up (Condie, 2004). Kenorland, Columbia, Rodinia, Gondwana and Pangaea (Fig. 7) are all examples of supercontinental assemblies in the geological past. The time scale of the supercontinental (Wilson) cycle is of the order of 300-400 Myr, and probably depends primarily on the time taken to incubate the sub-plate mantle sufficiently to inflate the supercontinent (Grigné *et al.*, 2007), cause break-up, and lead to migration of continental fragments to adjacent geoid lows. The Wilson cycle is therefore driven fundamentally by mantle circulation (Gurnis, 1988).

Extension of the supercontinent triggers the formation of the rift-drift suite of sedimentary basins, comprising continental rifts, continental rim basins, cratonic basins, failed rifts, proto-oceanic troughs, and passive margins. The subduction phase associated with late convergence triggers the formation of ocean trenches, accretionary wedge basins and forearc basins trenchwards of the magmatic arc, a range of basins in the retro-arc region, and strike-slip basins linked to oblique convergence. Continental collision is typified by foreland basin systems, including wedge-top deposition (De Celles & Giles, 1996; Ford, 2004). Consequently, certain basin types are common during particular phases of the Wilson cycle (Fig. 6). Cratonic basins, for example, tend to initiate at the rifting and break-up phase of the Wilson cycle (Fig. 7) when the plate is in a state of tension. In addition, the frequency of occurrence of basin types will depend on their long-term preservation by being shielded from tectonic recycling. This is an important consideration for Proterozoic basins, whose preservation potential is enhanced by incorporation into relatively rigid, stable, cratonic cores.

Neoarchaean-Proterozoic basin evolution; examples from chosen cratonic terranes

Kaapvaal craton

The nucleus of the Kaapvaal craton, formed through initial intra-oceanic tectonic processes and subsequent amalgamation of displaced oceanic and arc terranes, with significant granitoid magmatism in the later stages (model of de Wit et al., 1992), was stable but not yet fully cratonised by ca. 3.1 Ga. The craton comprises five known major terranes (Fig. 8a): Barberton-North and Barberton-South (BN and BS, accreted along the Barberton lineament, ca. 3.23 Ga); Murchison-Northern Kaapvaal (MNK, accreted to BN/BS along Thabazimbi-Murchison lineament [TML], ca. 2.9 Ga); Kimberley block (accreted onto assembled MNK-BN/BS, ca. 2.8-

2.72 Ga along the Colesburg lineament); Central Zone of the Limpopo mobile belt (accreted onto MNK from the "north" at ca. 2.65-2.7 Ga (Tinker et al., 2002; Zeh et al., 2009).

The lifespan of the Witwatersrand basin (Fig. 8a) essentially overlapped with the Neoarchaean cratonisation processes, and detritus was derived from the >3.1 Ga crust of the cratonic nucleus (cf., BN and BS) as well as the <3.1 Ga accreted juvenile gneiss-greenstone-granitoid terranes (MNK and Kimberley block), with granite pulses accompanying sedimentation episodes within the evolving depository (Robb and Meyer, 2005; Frimmel, 2005; references therein). A complex double foreland basin model is inferred with two convergent stress fields at about 100^0 to each other, reflecting the juvenile terranes accreting from both north and west. A proximal foredeep sub-basin accommodated the Witwatersrand Supergroup (WS) succession and the distal back-bulge sub-basin the Pongola Supergroup (PS) succession, with a persistent and emergent forebulge (however, not static in its position) separating the two and reflecting low subduction rates and inferred low subduction angles along the marginal accretionary zones (Catuneanu, 2001 and references therein) (Fig. 8b). Preservation of the back-bulge sub-basin may reflect the influence of dynamic topography (cf., Gurnis, 1988), although this influence is considered unimportant by Catuneanu (2001). The latter author relates the relatively short flexural wavelength of ca. 490 km to the newly cratonised nature of the Kaapvaal basement. Approximately coeval early volcanic rocks characterized the two sub-basins, succeeded by thermal subsidence in both as evidenced by ca. 2970-<2914 Ma starved basin foredeep marine deposits (West Rand Group, WS) which are correlated with shallow back bulge fluvial-marine storm deposits (Mozaan Group, PS) (Beukes and Cairncross, 1991; Robb and Meyer 1995; Catuneanu 2001). The transgression which established the West Rand seaway gradually gave way to highstand progradation, with a concomitant transition to the overfilled basin-type braided fluvial sandstones and subordinate auriferous conglomerates of the Central Rand Group (ca. 2894-2780 Ma), with no equivalent deposits in the back-bulge sub-basin (Robb and Meyer, 1995; Els 1998a and b; Catuneanu 2001; references therein). Eriksson et al. (2009) tentatively postulated that a mantle plume beneath the evolving craton may have influenced both geodynamic setting and enhanced primary greenstone sources of gold prior to Central Rand Group deposition, with reworking of this detritus through fluvial-shallow marine placer processes during Central Rand deposition.

The 2714-<2709 Ma Ventersdorp Supergroup (Fig. 8a) overlies the Witwatersrand Supergroup (WS) and surrounding cratonic lithologies unconformably. A significant (ca. 65-100 Myr) lacuna, in fact a megasequence boundary, separates the two supergroups (Eriksson et al., 2002 and references therein), during which tectonic shortening and erosion (either due to late stage continued subduction to N and W of Kaapvaal, or possibly, to early Ventersdorp thermal elevation) removed ≤1.5 km of WS stratigraphy (Hall, 1996). A mantle plume model (Hatton, 1995) is compatible with the largely volcanic Ventersdorp succession, and with its lower ca. 2 km thick Klipriviersberg Group (2714±8 Ma; Armstrong et al., 1991) flood basalts and basal komatiites (van der Westhuizen et al., 1991 and references therein). Ponding of mafic magma beneath the thinned sub-Witwatersrand basin lithosphere and a craton-marginal plume head are postulated (Eriksson et al., 2002). Subsequent crustal extension and resultant graben-type basins accumulated the immature clastic sedimentary and bimodal volcanic rocks, of the medial unconformity-based Platberg Group (c. 2709±4 Ma; Armstrong et al., 1991; van der Westhuizen et al., 1991) (Fig. 8c). The uppermost, widespread and sheet-like Bothaville and Allanridge Formations suggest thermal subsidence, with minor komatiites in the latter formation supporting a continued plume influence (van der Westhuizen et al., 1991; Eriksson et al., 2002; references

therein). Although undated, these uppermost Ventersdorp units may be related to a 2.66-2.68 Ga dyke swarm in NE Kaapvaal (Olsson et al., 2010); in addition, Ventersdorp-style rift-fills make up the so-called "protobasinal stage" of the younger Transvaal basin (Eriksson et al., 2001). This suggests possible "northern" movement of the abating plume influence due to "southerly"-directed plate tectonic movement of the craton.

The ca. 2.6-2.05 Ga Transvaal Supergroup (Fig. 8a) was deposited unconformably over all major preceding lithologies, crustal and supercrustal, and is preserved in three structural sub-basins, Transvaal and Griqualand West (South Africa) and Kanye (Botswana) (Eriksson et al., 2001 and references therein). A long-lived epeiric marine carbonate-banded iron formation platform advanced over much of the craton from the SW towards the NE (with several probably second-order transgressive-regressive cycles) from ~2642-2432 Ma; a lack of active tectonism is inferred with a predominant thermal sag basin model applied (Eriksson et al., 2006 and references therein). After a hiatus (80-200 Myr?), a second epeiric sea formed but this time largely clastic in its deposits and with thick shallow marine deposits alternating with thinner fluvial sedimentation, reflecting two episodes of rifting/volcanism and subsequent thermal subsidence in a sag basin setting. Cratonic architecture played a greater role in defining the three sub-basins, and unique stratigraphy and inferred history resulted for at least the Griqualand-West sub-basin (e.g., Eriksson et al., 2001). Each major epeiric succession, chemical and clastic, was preceded by local deformation (far-field tectonism?), concentrated along a curvilinear, ca. E-W orientated "palaeo-Rand anticline" near the centre of the craton. Continental freeboard of Kaapvaal is inferred to have been neutral, and elevated global sea levels related to raised crustal growth rates for the planet, probably produced the envisaged epeiric settings, with dynamic topography (cf., Gurnis, 1988) possibly also playing a role. Intrusion of the ca. 2.5 Ga Bushveld Complex in central-north Kaapvaal terminated Transvaal deposition and was succeeded by complex rifted basins around the intrusion, accommodating continental deposits of the Waterberg (Fig. 8a) and Soutpansberg Groups (ca. 2.05-1.7 Ga) (Bumby et al., 2012 and references therein), with increasing uniqueness in each sub-basin.

What is really of note for the Witwatersrand-Pongola retro-arc foreland basin system is that its evolution paralleled that of its host craton, and that the complex flexural foreland basin system, comprising northern and western marginal accretionary orogens, foredeep sub-basin, flexural bulge and southeastern back-bulge sub-basin, essentially covered the entire extant craton (Fig. 8a). This foreland system existed for ca. 190 Myr, based on available chronology. Of note for the Ventersdorp basin is that rifting was predominantly along NE-SW directions, unrelated to earlier major craton architecture, and that these fractures transgressed across the Colesburg lineament but not the TML (Fig. 8a); the latter limitation may reflect the ca. 2.65-2.7 Ga Limpopo orogeny. Once again, this basin affected a large part of the craton, which was by now stable enough not to suffer creation of new ocean floor within the rifts, and which maintained a fully continental character and elevated freeboard throughout its apparently short-lived evolution. Existing cratonic architecture essentially controlled Transvaal deposition, chemical and clastic, defining sub-basins and controlling lateral facies changes; cycles of relative sea level change were related at least in part to global eustasy, including a possible "magmatic slowdown" from ca. 2.45-2.2 Ga (Condie et al., 2009), which saw both the first global glaciation event and the "Great Oxidation Event" (Eriksson et al., 2013). Post—Bushveld, Waterberg-type basins were even more strongly controlled by existing cratonic architecture. For Kaapvaal, from ca. 3.1 – 1.7 Ga thus, basin evolution evolved from more unitary craton-scale depository styles, fully controlled by external tectonic-thermal influences (Witwatersrand and Ventersdorp) to where

cratonic architecture became predominantly responsible for sub-basins of increasingly diverging character (Transvaal and Waterberg).

Canadian shield

This brief overview includes only a small selection of Proterozoic basins of the Canadian shield. For more comprehensive earlier descriptions see Baer (1970) and Campbell (1981). The basement for some of the first Proterozoic basins was the "supercraton" Kenorland (Williams et al., 1991) which is interpreted to have formed by amalgamation of several greenstone belts (e.g., Card, 1990). It was during its break-up, near the beginning of the Proterozoic Eon, that plate tectonic and basin-forming processes in the Canadian shield began to approach modern dimensions and styles.

Perhaps the best example of an early Palaeoproterozoic depocentre related to break-up of Kenorland is the Huronian basin (1 in Fig. 9a). The Huronian Supergroup (~2.45 -2.2 Ga) is a thick (up to 12 km), dominantly siliciclastic succession that includes bimodal volcanic rocks near the base and contains evidence of three separate glaciations (in comparison, two are known within Kaapvaal's Transvaal depositories). The Huronian began as a rift basin but evolved into a passive margin at the time of deposition of the widespread glaciogenic Gowganda Formation (Young et al., 2001). Climatic oscillations, including the three glacial episodes, are ascribed to a negative feedback loop, initiated by "supercontinent" formation and controlled by weathering processes. The Huronian Supergroup also contains evidence of atmospheric oxygenation (the Great Oxidation Event). Following deposition of the Huronian Supergroup there is a depositional hiatus of about 300 Ma until the Penokean orogeny (~1.87 Ga), which marks ocean closure, accompanied by deposition and deformation of foreland basin deposits, preserved in the Sudbury basin and around Lake Superior, where they include the famous Superior-type iron formations (2 in Fig. 9a, b). Thus the Palaeoproterozoic rocks of the Great Lakes area can be seen as products of a "Wilson Cycle" of ocean opening and closure. Provenance of the Huronian sedimentary rocks was probably relatively local because it was constrained by the dimensions of Kenorland.

The Penokean and younger Palaeoproterozoic orogenies, such as the Wopmay, Talston-Thelon and Trans-Hudson in the NW and the extensive Yavapai to the south, contributed to consolidation of the first true supercontinent, Columbia or Nuna (Fig. 9b). Following these widespread orogenic events two large basins of late Palaeoproterozoic (1.85- 1.70) sedimentary (and volcanic) rocks were developed in the central part of the Canadian shield - the Thelon and Athabasca basins (3, Fig. 9a). The basal portion of these successions is strongly fault-controlled and locally derived but the more widespread, relatively flat-lying upper parts include far-travelled detritus and are remnants of a huge sand sheet (Rainbird and Young, 2009). These basins probably developed as a result of a regional phase of crustal stretching. There is also evidence of marine incursions (Hahn et al., in press, their fig. 11). An easterly provenance, was reported by Fahrig (1961) and Fraser et al. (1970) (Fig. 9a), and Young (1978) suggested that these basins are remnants of an ancient big river system that also fed deep repositories such as the Wernecke basin (3, Fig. 9a) to the west. The Wernecke Supergroup and correlatives to the NE were subjected to compressional orogeny (the Racklan/Forward orogenies). It was suggested by Furlanetto et al. (2012) that these events may be equivalent in age to the Mazatzal orogeny (Fig. 9a) but may record docking of Australia/Antarctica with the western part of North America during amalgamation of the supercontinent Columbia.

Following the break-up of Columbia and the widespread collision events of the Grenville orogeny the next phase of basin development is represented by the Mackenzie Mountains basin in the Cordilleran region and the Amundsen basin (5, Fig. 9a) in the western Arctic (Young et al., 1979). These basins may be expressions of long-lived crustal-scale tensional stresses and initial fragmentation of Rodinia that led to the rift-drift transition and formation of oceanic crust as inferred for the Neoproterozoic Rapitan (6, Fig. 9a), and similar basins farther south in the Cordilleran region, and in SE Australia (Preiss, 2000).

In the late Mesoproterozoic, at around 1100 Ma, during the Grenville collisional orogeny, a large, arcuate rift basin, almost 2,000 km long developed on the site of modern Lake Superior (Ojakangas et al., 2001). The fill of the Mid-Continent (Keweenawan) Rift basin (4, Fig. 9a, b) is a thick succession of basaltic lavas and continental-to-shallow marine sedimentary rocks. The northern "arm" of the triple junction is the Nipigon (mainly sedimentary) basin. Alternatively this basin may be interpreted as a back-arc tensional basin but its orientation and its configuration as a "triple junction" favour interpretation.as a failed attempt at ocean formation related to a mantle plume that developed near the NW margin of the Grenville orogen, where compressional events may have arrested its development. A similar but somewhat older (1.27 Ga) plume (Mackenzie hot spot of Fig. 9a) on the NW margin of the Canadian shield spawned one of the world's largest dyke swarms. Evidence for the origin of the Mackenzie dyke swarm, the associated Muskox intrusion and the Coppermine basalts as the result of a mantle plume and domal uplift was documented by LeCheminant and Heaman (1989).

The Neoproterozoic Amundsen and Mackenzie basins on the NW margins of the Canadian shield contain sedimentary rocks (including thick evaporites) that formed in warm shallow marine waters. Young (1978) speculated that some of the siliciclastic materials in these basins were derived from the Grenville mountains whose roots are preserved on the eastern seaboard of North America – a prediction later confirmed by detrital zircon geochronology (Rainbird et al., 1992). Thus part of the siliciclastic fill of these shallow marine extensional(?) basins had a very distant provenance – another increase in the scale of fluvial transportation systems.

The final basin-forming episode of the Proterozoic Eon involved a series of rift basins that once more preserve evidence of multiple glaciations and contain banded iron formations (Yeo, 1981), which had disappeared from the geological record for over a billion years (Fig. 9b). These rift basins are the result of a prolonged tensional episode that culminated in the break-up of Rodinia, as evidenced along the length of the North American Cordillera from Alaska to Mexico and in southeastern Australia. In many respects these events and rocks recall the history of the Palaeoproterozoic Huronian Supergroup.

The basins are shown in a temporal and tectonic context in Figure 9b. Basin evolution in North America generally involved an increase in scale with time, as their source areas and fluvial sediment conduits (Fig. 9a) expanded. Modern-style plate tectonics began to manifest itself clearly in the Huronian Supergroup. The planet went through dramatic climatic oscillations, probably related to emergence of the first "supercraton" in the Canadian shield. These events were accompanied by, and possibly triggered atmospheric oxygenation (the Great Oxidation Event). Many younger Proterozoic basins illustrate the increasing scale of fluvial systems as materials were shed from distant late Palaeoproterozoic and late Meso- to Neoproterozoic orogens. The Keweenawan basin and the Mackenzie hot spot and associated dyke swarm record ancient (1.27- 1.1 Ga) aborted attempts at ocean formation, deep within Rodinia. The final Proterozoic basins contain evidence of a second series of glaciations and a new oxygenation

event, this time leading to the Cambrian "explosion" of metazoan life forms as the Proterozoic Eon came to an end in a manner that matched its dramatic beginning.

Brazilian shield

The Precambrian nucleus of South America, to which Patagonia and the Andean terranes accreted during the Phanerozoic, was amalgamated through a series of diachronous collisions during the Ediacaran and Cambrian periods, between 635 and 520 Ma. The internal and relatively stable portions of the larger plates involved in the Ediacaran collisions are represented by four cratons, namely Amazon, São Luis, São Francisco and Rio de La Plata-Paranapanema, whereas plate margins, intra-oceanic arcs and micro-continents make up the Ediacaran network of the so called Brasiliano orogenic systems (Fig. 10) (Brito Neves et al. 1999; Almeida et al., 2000; Alkmim et al. 2001). Cratons and Ediacaran orogenic belts are exposed in three distinct morphotectonic domains of the continent, the Guyanas, Central Brazil and Atlantic shields. These domains are collectively referred to as the Brazilian shield (Fig. 10). Proterozoic sedimentary basins with preserved architectures and significant thicknesses of fill successions occur on the Amazon and São Francisco cratons. However, in order to provide a representative overview of Proterozoic basin evolution for the Brazilian shield, this summary includes examples of basins and sedimentary sequences occurring on both the cratonic and extracratonic domains.

The Amazon craton, one of the largest and lesser known Precambrian provinces in the world, consists of an Archaean core and a series of terranes accreted between 2.2 and 1.1 Ga (Tassinary et al., 2000; Santos et al., 2000; Santos, 2003). Proterozoic basins of the Amazon craton developed during one of the following succession of tectonic events: (i) continental plate individualization and their subsequent involvement in the assembly of the Palaeoproterozoic supercontinent Columbia between 2500 and 1900 Ma; (ii) intraplate basin-forming episodes accompanied by voluminous anorogenic magmatism, between 1900 and 1600 Ma; (iii) Columbia break-up, followed by a series of accretionary events between 1800 and 1000 Ma, which ultimately led to the assembly of Rodinia by the end of the Mesoproterozoic; (iv) development of passive margins associated with the dispersal of Rodinia at around 700 Ma; (v) continent convergence and collision during the assembly of West Gondwana by the end of the Neoproterozoic (Tassinary et al., 2000, Santos et al., 2000, Santos, 2003; Schobbenhaus and Brito Neves, 2003; Fuck et al., 2008).

Large Proterozoic basins cover a substantial part of the Archaean Central Amazonian province. The oldest among these basins hosts the 1875 Ma Roraima Supergroup, an up to 3km-thick package of fluvial, deltaic and shallow marine sediments (Gibbs and Barron, 1993; Santos et al., 2003). Exposed in the 3000m-high table mountains that mark the borders of Brazil, Venezuela and Guyana, the Roraima Supergroup is portrayed as a foreland basin-fill succession, shed from a Palaeoproterozoic orogenic belt developed along the north and northeastern margin of the Central Amazonian Province (Santos et al., 2003). The central and southwestern portions of the Central Amazonian province are partially covered by acid and intermediate volcanic rocks of the 1880 Ma Uatumã magmatic event, viewed by Brito Neves (2011) as comprising a large igneous province (LIP). These volcanic rocks are intercalated locally and covered by thick sequences of continental sedimentary rocks, thereby defining a series of depocentres that might have extended over an area of 1,500,000 km^2 (e.g., Schobbenhaus and Brito Neves, 2003).

The São Francisco craton located in eastern Brazil consists of an Archaean nucleus and segments of a 2.1 Ga Palaeoproterozoic orogen (Teixeira et al., 2000; Almeida et al., 2000; Barbosa and Sabaté, 2004). Its oldest Proterozoic successions comprise the Minas and Itacolomi basins, which document a complete Wilson cycle operating at the beginning of the Palaeoproterozoic, between 2.6 and 2.0 Ga (Dorr, 1969; Marshak and Alkmim, 1998). Initiated as a rift-fill with alluvial sandstones and conglomerates shed from Archaean sources of the craton interior, the Minas basin evolved into a passive margin in the course of the Great Oxidation Event (ca. 2.4-2.3 Ga). This stage is marked by the deposition of banded iron formations and shallow water carbonates dated at 2.42 Ga (Babinski et al., 1995), which also seem to record a glacial episode (Alkmim and Martins-Neto, 2012). A collision involving a large magmatic arc and micro-continents led to the amalgamation of the Archaean nuclei of the São Francisco and Congo cratons at ca. 2.1 Ga. A thick package of turbiditic sandstones and conglomerates derived from the inverted continental margin and a colliding arc accumulated in the Minas basin. Alluvial sandstones and conglomerates of the Itacolomi Group, deposited in intermontane basins during extensional collapse, mark the end of the Wilson cycle (Machado et al., 1996; Alkmim and Marshak, 1998). Immediately after their amalgamation, the São Francisco and Congo nuclei were probably incorporated into the large Atlantica (super)continent.

The Espinhaço basin records a long succession of intraplate basin-forming episodes accompanied by anorogenic magmatism that affected the São Francisco-Congo craton between 1.75 and 0.9 Ga. The development of this basin started with a major extensional event in the Staterian Period. Fluvial, lacustrine and aeolian sediments interbedded with bimodal volcanics were deposited in a system of rift basins, presently exposed in the craton interior and along the marginal Brasiliano belts (Brito Neves, 2011; Uhlein et al., 1998; Martins-Neto, 2000). Renewed pulses of extensional tectonism and magmatism caused reactivation and expansion of the Staterian depocentres at ca. 1.5, 1.4, 1.2, and 1.0 Ga, resulting in a long-lived rift-sag basin system (Danderfer et al., 2009; Chemale et al., 2012; Alkmim and Martins-Neto, 2012). Perhaps because of some specific climatic conditions and continuous sediment recycling, thick packages of aeolian, alluvial, and shallow marine quartz arenites were stored in the Espinhaço basin system.

The São Francisco craton and its fringing Brasiliano belts do not display the effects of a Grenvillian collisional event. Together with the Congo craton, the São Francisco apparently remained in the periphery of Rodinia, or as an isolated continental mass during the Meso-Neoproterozoic transition (e.g., Weil et al., 1998; Pisarevsky et al., 2003). At around 850 Ma, the craton experienced another extensional event, which led to reactivation of pre-existing interior basins, and sometime later in the Cryogenian Period between 850 and 740 Ma, to the accumulation of the thick sequence of glaciomarine diamictites, sandstones, pelites, iron formations and minor carbonates of the Macaúbas passive margin basin (Uhlein et al., 1999, Martins-Neto et al., 2001; Pedrosa-Soares et al., 2001, 2008). The Macaúbas basin was caught up in the Brasiliano orogenic front during the assembly of West Gondwana at around 570 Ma and was involved in the Araçuaí orogenic belt that bounds the São Francisco craton to the southeast. Later in the course of this process, the São Francisco craton was almost entirely occupied by shallow marine waters and progressively converted into foreland depositional sites. Carbonate, pelite and subordinate conglomerates and sandstones of the Ediacaran Bambuí Group record the youngest Proterozoic basin-forming event in the cratonic domain (Castro and Dardenne, 2000; Alkmim and Martins-Neto, 2012).

Australian continent

Basins developed following the accretion of crustal elements of the North Australian, South Australian, and West Australian cratons during the amalgamation of the supercontinent Columbia. Amalgamation of individual tectonic elements occurred over a relatively short interval between ca. 1880 Ma and ca. 1800 Ma as continental ribbons (Betts et al., 2002; Korsch et al., 2012), juvenile arc terranes (Sheppard et al., 1999; Kirkland et al., 2013), and cratons accreted. The post-accretion Palaeoproterozoic basin record is preserved over large tracts of the Australian continent (Fig. 11a-d). These depositories have been extensively studied in the Mount Isa Inlier and the McArthur Basin (Fig. 11a) where there is a record of more than 250 million years of basin formation (Jackson et al., 2000; Southgate et al., 2000) (Fig. 11e). However, components of the basin systems are preserved over a larger area of the Australian continent and include the Georgetown Inlier, Granites-Tanami Block, Curnamona Province, Gawler Craton, Davenport Province, and Arunta Inlier (Fig. 11).

The palaeogeography of the Australian Proterozoic Basins is constrained by palaeomagnetic data and tectonic correlations that show Australia and Laurentia were fellow travellers between ca. 1850 Ma and 1650 Ma (Idnurm and Giddings, 1995; Karlstrom et al., 2001; Betts et al., 2008; 2011). During this interval, the southern margin of Australia and Laurentia was a complex convergent margin characterized by episodic accretion and subduction roll-back (Betts et al., 2011) (Fig. 11f-h), leading to interpretations that the Palaeoproterozoic superbasins of Australia formed in a large extension-dominated, continental back-arc region (Giles et al., 2002), although alternative interpretations include dynamic subsidence related to convergence on the southern continental margin (Scott et al., 2000) and a Basin-and-Range style tectonic setting (Gibson et al., 2008). The continental back-arc models are supported by the sensitivity of the basin events to established plate margin processes. For example, major episodes of basin inversion, basin uplift and unconformity development are temporally linked with major episodes of accretion along the southern margin of the continent (Giles et al., 2002; Betts et al., 2003; Betts and Giles, 2006) and major inflections and bends in Australia's apparent polar wander path (Idnurm and Giddings, 1995). A relatively small oceanic basin resulting in the separation of Australia and Laurentia is interpreted to have formed along the eastern margin of the continent at ca. 1660-1650 Ma (Betts et al., 2003; Lambeck et al., 2012). The complex palaeogeography has resulted in an equally complex and protracted basin history in which four basin-forming events are superimposed.

The earliest evidence for post-Columbia basin development is preserved in the Granites-Tanami Block, Arunta Inlier, and the Tennant Creek - Davenport Province (Fig. 11e). Sedimentation in these regions initiated at ca. 1840 Ma and comprises the ~5 km thick Tanami Group (Granites-Tanamoi Block), which records two cycles of upward-fining, turbidite-dominated successions (Bagas et al., 2008). The Tanami Group is correlated with shallow marine to sub-aerial siliciclastic sedimentary rocks and bimodal volcanic rocks of the Ooradidgee Group (ca. 1840 Ma) and layer-cake fluviatile to shallow marine siliciclastic rocks of the Hatches Creek Group (ca. 1820–1800 Ma) (Claoué-Long et al., 2008), which are preserved in the Tennant Creek - Davenport Province. The deformed and metamorphosed remnants of marine clastic sediments and felsic and mafic volcaniclastic rocks (Ongeva Packages) in the Arunta Inlier were deposited in the same basin (Claoué-Long et al., 2008).

The second basin forming event, well represented in the Mount Isa Inlier and the McArthur Basin (Fig. 11), occurred between ca. 1800 Ma and 1740 Ma (Fig. 11e). In the Mount Isa Inlier this basin is termed the Leichhardt Superbasin (Jackson et al., 2010) in which three second-order super-sequences accumulated (Neumann et al., 2006) during episodic rifting and post-rift thermal subsidence (O'Dea et al., 1997). The basal Leichhardt Superbasin-fill comprises ~5km of alluvial sheet, braided river, marginal lacustrine and marine deposits (Eriksson et al., 1993) (Guide Supersequence; Nuemann et al., 2006). Correlative stratigraphy in the McArthur Basin includes the braided river deposits of the Westmoreland Conglomerate (Wygralak et al., 1988). Eight kilometres of tholeiitic continental basalts (ca. 1780-1775 Ma: Eastern Creek Volcanics) were emplaced during a 5-10 My period within a N-S trending, linear rift axis. These are overlain by the Myally Subgroup, which is dominated by shelf deposits with transient emergence represented by playa lake deposits (Eriksson et al., 1993). Correlative flood basalts in the McArthur Basin (Seigal Volcanics) are intercalated within dominantly fluvial to intertidal packages of the lower Tawallah Group (Rawlings, 1999). In the eastern Mount Isa Inlier, basin development was characterised by bimodal volcanism and clastic shallow marine sedimentation. The transition to ca. 1750-1740 Ma post-rift sedimentation is represented by the storm-, tide-, and wave-dominated marine shelf and continental facies quartzites, which were deposited during active extension (Potma and Betts, 2006). These are overlain by calcareous siltstone and limestone (Quilalar and Corella formations). Correlative basinal successions in the southern and eastern Gawler Craton, are dominated by ca. 1790-1780 Ma fine-grained schist and BIF (Cleve Group) (Szpunar et al., 2011), ca 1755 Ma felsic volcanics and fluvial sediments (Moonabie Formation), and finer-grained, marine siltstone and shale of the ca. 1760-1740 Ma Wallaroo Group in the Yorke Peninsula, suggesting the basin system deepened to the east (Fig. 11b). Meta-sedimentary lithologies in the Nawa Domain and the Peake and Denison Inlier of the Northern Gawler Craton record a phase of basin development between ca. 1750 and 1730 Ma (Payne et al., 2009). The ~5 kilometre thick Earaheedy Basin-fill (Fig. 11b) on the northern Yilgarn Craton records continentally derived clastic and carbonate shelf deposits overlain by shallow marine to coastal carbonate and evaporate lithologies and deposition of chert and iron formations (Pirjano et al., 2009). In the Arunta Inlier, the carbonate-rich succession of the Cadney Package and the clastic-dominated successions of the Reynolds Package (ca. 1780 Ma) and the Ledan Package (ca. 1760-1740 Ma), are correlated with the Leichhardt Superbasin.

Between ca. 1740 and 1710 Ma the basin evolution of North Australia was restricted to the deposition of fine-grained sandstone facies deposited in a storm-dominated marine shelf environment, black shale, and dolomitic siltstone–mudstone facies deposited in hypersaline conditions (Wollogorang Formation) at ca. 1730 Ma. Black Shales within the Wollogorang Formation exhibit Black Sea-type iron enrichment, high DOP values, and generally uniform S-isotope compositions for pyrites, suggesting a euxinic basin, possibly with open ocean conditions (Shen et al., 2002). If this interpretation is correct, the open ocean must have existed to the west or the north because regions to the east (e.g. Mount Isa) were undergoing basin inversion and uplift (Betts, 1999), and terranes to the south (Arunta Inlier and Gawler Craton) were experiencing orogenesis as the Gawler Craton re-accreted onto the southern margin of the Australian continent.

The Calvert Superbasin is the third cycle of basin development between ca. 1710 Ma and 1670 Ma (Fig. 11e). Two second-order cycles of between 1 and 3 km thickness are preserved in the western Mount Isa Inlier. Fluvial sedimentation and rift-related, bimodal volcanic successions were deposited in an evolving half-graben at ca. 1710-1690 Ma (Betts et al., 1999;

Gibson et al., 2008). Deepening of the basin between ca. 1690 Ma and 1670 Ma resulted in fluviatile to shallow marine sandstone, siltstone, and carbonate, as well as deep marine, carbonaceous turbidite successions farther east, which most likely records a shift in the basin depocentre (e.g., Soldiers Cap Group) (Gibson et al., 2008) (Fig. 11c). In the McArthur Basin aerially restricted clastic sandstones were deposited in a shallow marine to fluvial environment within the Walker Fault Zone (Goyder Package; Rawlings, 1999). In the central Gawler Craton, shallow marine or lacustrine clastic sandstone and subsequently recrystallised quartzite with minor chemical sediments were deposited within a restricted fault-controlled basin (Daly et al., 1998). The Calvert Superbasin cycle is recorded in the Lower Willyama Supergroup (ca. 1715-1670 Ma) in the Curnamona Province. These rocks are intensely deformed and metamorphosed (up to granulite facies) and have been interpreted to have been deposited in an epicontinental rift environment (Conor and Preiss, 2000). The protoliths to these ca. 1715 Ma gneissic rocks are thought to have been deposited in shallow marine and sebkha environments, characterised by oxidised saline basin conditions (Conor and Preiss, 2008). The presence of bimodal igneous suites is consistent with the interpreted rift tectonic setting. Emergence of the basin in the east was coincident with deposition of shallow marine to fluviatile sediments of the Thackeringa Group in the west, between ca. 1705 Ma and 1700 Ma (Conor and Preiss, 2008). A marine transgression led to marine shelf clastic and chemical sediments, coupled with extensive bimodal magmatism, being deposited during continued rifting (Conors and Page, 2008). This transgression also marks a shift in basin redox conditions with reduced conditions prevailing. Fluvial to shallow marine depositional environments occurred in the central Gawler Craton at ca. 1715 (Eba Formation; Howard et al., 2011). In the far east of the Australian continent (Georgetown Inlier), the Calvert Superbasin phase is characterised by the deposition of fine-grained, deep-water turbidites and carbonate sediments (Withnall et al., 1988) (Fig. 11c). The broad pattern of sedimentation during the Calvert Superbasin cycle indicated that extensional basin networks may have been aerially restricted in the interior of the continent with deeper water environments along the eastern margin of the continent, which possibly faced an ocean. Along the southern margin of the Arunta Inlier are laminated Fe-rich and manganiferous sedimentary rocks and calc-silicates, which may have formed at the passive margin of the allochthonous Warumpi Province.

The transition from the Calvert Superbasin cycle to the Isa Superbasin cycle (ca. 1668-1595 Ma) was characterised by the development of mid-crustal detachment faults and granite emplacement, possibly reflecting metamorphic core complex development (Gibson et al., 2008) at ca. 1675-1665 Ma, coincident with a 20 My hiatus in sedimentation in the Curnamona Province. The cumulative thickness of the Isa Superbasin-fill is highly variable however, seven second-order sequences having been identified, each varying in thickness between 1 and 3 kilometres (Southgate et al., 2000). This basin system extended from the Curnamona Province through to the Birrindudu Basin and possibly the Kimberley Basin in northwest Australia (Fig. 11d). The superbasin-fill succession is extensively studied in the Mount Isa Region and in the McArthur Basin where significant sediment-hosted Pb-Zn mineralization occurs.

The onset of sedimentation is marked by rapid subsidence in which several third-order cycles of fine-grained sandstone, siltstone, and carbonaceous shale of the Mount Isa Group and lower parts of the McNamara Group were deposited under shallow water conditions (Southgate et al., 2000). In the McArthur Basin, the base of the Isa Superbasin-fill is characterised by fluvial sandstone and continental red beds. At ca. 1555 Ma, shallow water fine-grained siliciclastics and carbonates prevailed in the western Mount Isa Inlier, whereas in regions to the northwest,

deposition occurred in fluvial and shallow water environments (Southgate et al., 2000). These units temporally correlate with the Paragon Group (Curnamona Province) and fluvial to marine successions of the aerially restricted Tarcoola Formation (central Gawler Craton; Daly et al., 1998) and the Birrindudu Basin, which is characterised by fluvial sandstones passing up into a preserved marginal shelf environment. The overlying subtidal carbonate blanket (Lady Loretta Formation) contains black shale horizons and was developed on a regional platform. In the McArthur Basin, dolostone with minor fine-grained siliciclastics record shallow to moderately deep-water conditions deposited within the meridional troughs or rifts. These successions indicate ferruginous basin conditions that suggest anoxic basins prevailed (Shen et al., 2002; Planavsky et al., 2011) between ca. 1650 Ma and 1640 Ma during a period when there was likely to have been an open ocean east of the Australian continent. The deepest part of the basin occurred to the east (eastern Mount Isa Inlier, Curnamona Province, and Georgetown Inlier), where sedimentary successions are dominated by outer shelf and deep water sediments (Gibson et al., 2011; Conor and Preiss, 2008). Lambeck et al. (2012) also documented a fundamental shift in Sm-Nd isotope signatures of the North Australian Basins at ca. 1655 Ma marked by an increase in material derived from juvenile crustal sources, possibly reflecting passive margin volcanism along the eastern margin of the Australian continent.

Seismic data suggest that there is a major erosional surface within the platform carbonate facies (Southgate et al., 2000). This surface records incision that was related to tectonic uplift, coincident with the accretion of the Warumpi Province along the southern Arunta Inlier (Scrimgeouret al., 2005) at ca. 1645-1640 Ma. Renewed sedimentation was marked by increased flux of siliciclastics followed by regional transgression and several second- and third-order cycles, marked by fault-controlled deep marine and shelf sedimentation with transient emergence, in both the Mount Isa Inlier and the McArthur Basin (Southgate et al., 2000; Rawlings, 1999); this was followed by turbidite and shelf carbonate sedimentation in Mount Isa, and siliciclastic shelf deposition in the McArthur Basin. The upper parts of the superbasin-fill comprise sand-rich submarine fan and fluvial clastic deposits that temporally overlap with the Isan Orogeny (ca. 1595 Ma) and which appear to truncate, and are fault-controlled by, strike-slip or wrench faults (Scott et al., 1998).

Following approximately 100 million years of episodic orogenesis between ca. 1600 Ma and 1500 Ma (Betts et al., 2009) renewed basin development is recorded sporadically throughout the Australian continent. Superimposed on the McArthur Basin-fill by a regional unconformity, the Roper Group (Roper Superbasin) was deposited at ca. 1430 Ma (Jackson et al., 1988) within an epicontinental basin (Rawlings, 1999). This laterally extensive package varies in thickness with the thickest sections (~3 km) preserved in the Beetaloo Sub-basin. The Roper Group is laterally extensive and comprises quartz arenite, siltstone, shale, with minor carbonate and laminated shelf mudstone intervals, deposited as a predominantly shallow-marine clastic succession. In the Gawler Craton, an aerially restricted package of dominantly fluvial red beds of the Pandurra Formation was deposited within the intracratonic Cariewerloo Basin (Wilson et al., 2010). The timing of this basin is poorly constrained however, overprinting criteria and Rb–Sr geochronology indicate deposition between ca. 1550 Ma and 1424 ± 51 Ma. The tectonic environment of these basins is poorly resolved but is coincident with a period of continental re-amalgamation and associated rifting (Giles et al., 2004).

Northern North China craton

The North China craton (NCC) basement was formed as a result of the amalgamation of its western and eastern blocks along a so-called Trans-North China orogen around 1.85 Ga (Zhao et al., 2003). The rifting commenced since the late Palaeoproterozoic, mostly along the northern and southern margins of the NCC, and was associated with sedimentation and magmatism. Different portions of the NCC experienced distinct tectono-sedimentary evolution during the period from the late Palaeoproterozoic to middle Mesoproterozoic (Lu et al., 2008). The upper Mesoproterozoic is missing, although extension-related magmatism took place in the northern NCC in the time interval from 1.35 to 1.32 Ga (Zhang et al., 2009; Shi et al., 2012). The Neoproterozoic strata are preserved in a few localities along the NCC southern and northern margins, but it remains unclear what the tectonic settings were for the Neoproterozoic deposits. This brief review focuses on the Palaeo- and Mesoproterozoic development of sedimentary basins of the northern NCC.

The northern NCC experienced strong lithospheric extension in the late Palaeoproterozoic, as registered by widespread ca. 1.78 Ga mafic dike swarms (Peng et al., 2005) and 1.75–1.68 Ga A-type granitoid intrusions (Zhang et al., 2007) (Fig. 12A). The magmatism is considered to have resulted from asthenospheric upwelling (Peng, 2010), which presumably also led to widespread topographic doming and erosion in the northern North China craton. Rift basins did not develop in this period of time. The Palaeo- and Mesoproterozoic successions are divided into the Changcheng, Nankou, and Jixian Groups (Fig. 12A). The Changcheng Group was deposited across the Archaean to early Palaeoproterozoic crystalline basement, and its initial age is considered to be ca. 1.65 Ga for it overlies felsic dikes dated at ca. 1.67 Ga (Li et al., 2011). The Dahongyu Formation of the Nankou Group contains abundant potassium-rich volcanics, zircons from which have yielded ages of 1622–1625 Ma (Lu et al., 2008). Two zircon U-Pb ages have been obtained, one of 1559 ± 12 Ma by SHRIMP and another, 1560 ± 5 Ma by LA-ICP-MS (Li et al., 2010) from tuff layers of the Gaoyuzhuang Formation (top of Nankou Group), indicating that deposition of this unit may have begun at ca. 1600 Ma, the time of transition from the Palaeo- to Mesoproterozoic. The Jixian Group is comprised predominantly of carbonate rocks, and the overlying Xiamaling Formation consists of black mudrocks (Fig. 12A). The volcanics in the Tieling Formation at the top of the Jixian Group yield zircon ages of 1437 ± 21 Ma (Su et al., 2010), indicating that this group was deposited in the early Mesoproterozoic. The Xiamaling Formation was previously assigned as a Neoproterozoic unit (cf. Lu et al., 2008), but recent dating of its tuff interlayers gives a zircon age of 1366 ± 9 Ma (Gao et al., 2008).

Palaeoproterozoic rift basins are well recorded by the Changcheng Group in the eastern portion of the northern NCC (Meng et al., 2011), also called the Yanshan-Liaoxi rift zone in the literature. The rifting interpretation is inferred from both the occurrence of volcanics and thick accumulations of sediments within narrow zones in the northern NCC. Subsidence and sedimentation were controlled by normal faults, particularly evident for the Changcheng Group (He et al., 2000). Extensional faulting waned when the Nankou Group developed because the Dahongyu deposits are relatively thin and show gradual change of stratigraphic thickness. The rifting might have ended by the beginning of the Mesoproterozoic, as suggested by widespread distribution and insignificant variations in thickness of the Gaoyuzhuang Formation that had transgressed into the middle of the NCC (Fig. 12A). The Nankou Group is accordingly interpreted as post-rift sequences (Meng et al., 2011). Widespread shallow-marine clastic and carbonate facies of the Mesoproterozoic Nankou and Jixian Groups in the north and central parts of the NCC are regarded as deposits formed on a passive continental margin (Fig. 12A). The

Bayan Obo–Zhaertai rift basins in the western portion of the northern NCC seem to have undergone similar tectono-sedimentary processes during the Palaeo- and early Mesoproterozoic (Meng et al., 2011), but their detailed history is less understood.

In general, the northern NCC experienced a two-stage evolution of synrift and post-rift subsidence, represented by the Changcheng and Nankou Groups, respectively. The two distinct sequences are separated by a transgressive unconformity and its correlative conformity in the basin interior. Two possibilities exist for cessation of active rifting during the transition from the Changcheng to Nankou Groups, the overall termination of continental extension or the lateral shifting of the extensional zone. It is evident that post-rift successions are composed of both the Nankou and Jixian Groups and are characterized by wide distribution and greater thickness of shallow-marine clastics and carbonates. This fact implies a broad subsidence and a prolonged depositional history, which might be caused by thermal contraction of subcrustal materials heated only during the synrift stage. Sudden lateral shifting of active extension might be a possible reason for cessation of the rifting in the northern NCC. In addition, the transgressive unconformity identified beneath the Dahongyu and Gaoyuzhuang Formations can also be regarded as the breakup unconformity in the context of regional tectonic evolution (Meng et al., 2011). If the identification of the breakup unconformity is correct, its age could be used to infer the timing of dispersal of the North China craton from adjacent continents, although the pre-existing Palaeo-Mesoproterozoic oceanic crust has not been preserved. The breakup unconformity was time-transgressive, and the time range can be readily inferred from ages of the Dahongyu and the Gaoyuzhuang sequences. It is therefore reasonable to infer that the breakup unconformity was generated in the time interval from 1630 Ma to 1560 Ma, and thus the drifting of the North China craton should have begun around 1600 Ma. This age estimate for the drift of the North China continent is coincident with that suggested for the breakup of Columbia (Zhao et al., 2003). It is, however, uncertain which continents were originally linked with the northern NCC.

Figure 12B presents a model for the tectono-sedimentary evolution of the northern NCC during the period from late Palaeo- to Mesoproterozoic time. The Columbia supercontinent formed around 1900 Ma and then began fragmenting (Zhao et al., 2003), leading to widespread extension and magmatism in the northern NCC. The rift basins began developing around 1.65 Ga, and sedimentary processes were controlled by normal faults and accompanied by volcanism (Fig. 12B-a). Due to oceanward migration and localization of active crustal stretching, normal faulting became inactive within the northern NCC (Fig. 12B-b). Post-rift subsidence, driven by thermal decay, commenced, and brought about expansion of original rift basins. The resulting marine transgression led to the Dahongyu transgressive deposition over Archaean basement rocks (Fig. 12B-b). The continent broke up eventually, and seafloor spreading led to the fragmented continental blocks drifting away from each other (Fig. 12B-c). The northern NCC then evolved gradually into a passive continental margin in the Mesoproterozoic. The Gaoyuzhuang Formation represents early deposits of the passive continental margin, typified by widespread occurrence of its sheet-like basal clastics caused by transgression. The passive-margin tectono-sedimentary setting persisted in the early Mesoproterozoic and was responsible for deposition of widely-distributed shallow marine facies of both the Jixian Group and, elsewhere, the upper parts of the Bayan Obo and Zhaertai Groups. The Xiamaling Formation probably formed in another phase of crustal extension in consideration of occurrence of abundant coeval volcanism and subsequent extension-related mafic and A-type intrusions (Fig. 12A).

Discussion and conclusion

In this paper we have examined briefly Neoarchaean – Neoproterozoic basins from the Kaapvaal craton, Canadian shield, Brazilian shield, Australian continent and North China craton, as examples to illustrate the inherent complexity of the natural record against the basin classification schemes discussed in the first part of the paper. The vast majority of basin classification schemes rely essentially on a plate tectonic basis and thus inherently also involve the supercontinent cycle (Figs. 1-7). While the antiquity of the latter has been the subject of considerable debate (e.g., Rogers and Santosh, 2004), many would agree that at about 2.0 – 1.8 Ga, the supercontinent cycle had become predominant if not pervasive on the planet (e.g., "Nena"/"Nuna", Bleeker, 2003; "Arctica", Eyles, 2008; "Colombia", Santosh, 2010). In this paper the Kaapvaal basins precede this apparently global piercing point, while those from the Australian and North China cratons post-date it; depositories examined from the Canadian and Brazilian shields span almost the entire Neoarchaean – Neoproterozoic period examined through the chosen examples. While it would be beyond the scope of this paper to review all global basins of this antiquity, there is perhaps a certain value in examining some of the generalizations to emerge from the relatively small set discussed here.

Basin types and geneses identified versus basin classification schemes

The 25 basins (cf. superbasins, basin sets) briefly examined in our examples have thus far been given labels based on the descriptions and interpretations provided, rather than being assigned to categories within the more formal classifications (Figs. 1-7) given prior to these case studies: foreland basins (Witwatersrand; Penokean basin set; Roraima; upper Minas-Itacolomi; Bambui); plume-related rift basins (Ventersdorp; Keweenawan; Uatuma); thermal sag basins (lower Transvaal); rift-sag basins (2 in upper Transvaal); cratonic rift-sag basins (Thelon; Athabasca; Espinhaco; Leichhardt superbasin; Isa superbasin); rift basins (Waterberg; Rapitan basin set; Macaubas; Calvert superbasin); rift-drift basins that became passive margins (Huronian; Lower Minas; North China); rift-drift failed ocean basins (McKenzie Mountains; Amundsen). Even these relatively simple classifications inherently encompass complexity: for example, (1) the Witwatersrand is a retro-foreland basin system loaded by two orogenic belts; (2) two of the five foreland basins identified enable interpretation of concomitant Wilson cycles (Penokean set; upper Minas-Itacolomi); (3) the three Australian superbasins probably formed within an overall continental back-arc setting, which probably favoured their preservation; (4) a third possible Wilson cycle can be postulated for the preserved ca. 2.7-2.3 Ga record on Kaapvaal, encompassing evidence for initial rifting (Ventersdorp), succeeding passive margin development (lower Transvaal) and terminal orogeny (at "ocean closure"), within the time gap separating upper and lower Transvaal depositories, with postulated local intermontane rifts accommodating glacial deposits (discussion in Melezhik, 2013).

The informal basin classifications arising from the case studies above can readily be grouped into fewer categories: foreland basins; rift basins (plume- and non-plume – related); intracratonic sag basins (rift-sag, cratonic rift-sag and thermal sag basins; logically, also, the rift-drift failed ocean basins above); cratonic-margin located rift-drift basins (that evolved into passive margins). However, the allocation of a basin to a specific type and formal classification depends essentially

on the inherent complexity (or otherwise) of the chosen scheme, and deciding whether a rift-sag basin belongs with the rift group or not remains at least somewhat elusive and perhaps even rather pointless at the individual basin scale. With a very long-lived extensional reactivated rift basin set such as the Espinhaço from the Brazilian shield, or with all three of the Australian superbasins, problems with choice of classification scheme and allocation of specific name therein, will also arise, depending partly on scale (from individual basin within a larger depositional assembly to an entire superbasin) or on changes or the lack thereof over long time periods.

Below we assign each of the 25 basins we used as case studies within two of the classification schemes presented in the first part of the paper: firstly to Kingston *et al.*'s (1983a) more descriptive scheme as modified by Allen & Allen (2013) (Fig. 3); secondly, to the more genetically-based scheme of Allen & Allen (2013) predicated on subsidence mechanisms (Fig. 5), respectively:

Our foreland basin examples:
Witwatersrand – intracontinental foreland; retro-foreland basin;
Penokean basin set – retro-foreland basin; retro-foreland basin;
Roraima – intracontinental foreland; retro-foreland basin;
Upper Minas-Itacolomi – intermontane basins; "intermontane" retro-foreland basin?;
Bambui – intracontinental; pro-foreland basin.
Our plume-related rift basin examples:
Ventersdorp – continental rift; continental rift;
Keweenawan – failed rift?; failed rift;
Uatuma – continental rift; continental rift.
Our thermal sag basin examples:
Lower Transvaal – cratonic sag; cratonic basin.
Our rift-sag basin examples:
2 in upper Transvaal – failed rift?; failed rift?.
Our cratonic rift-sag basin examples:
Thelon – continental rift; continental rift;
Athabasca – continental rift; continental rift;
Espinhaco – continental rift developing into cratonic sag?; continental rift into cratonic basin?;
Leichhardt superbasin – (rift-sags within) continental back-arc; continental back-arc;
Isa superbasin – as above; as above.
Our rift basin examples:
Waterberg – continental rift; continental rift;
Rapitan basin set – rift (prior to passive margin); passive margin
Calvert superbasin – continental rift; continental rift.
Our rift-drift to passive margin basin examples:
Huronian – passive margin; passive margin;
Lower Minas – passive margin; passive margin;
North China – passive margin (all three with initial rifts); passive margin;
Macaubas – passive margin; passive margin.

Our rift-drift failed ocean basin examples:

McKenzie Mountains – failed rift?; failed rift?;
Amundsen – failed rift?; failed rift?.

As can be seen in the summary above, there is little difference in basin type and name given within the two schemes, even though the first one emphasizes a more rigid descriptive plate tectonic framework for classification (Fig. 3), and the second scheme relies mainly on mechanism of basin formation and evolution (Fig. 5). Uncertainties above are shown with question marks. While the more formal classification schemes evolved over the years have a place within the science of basin analysis, each scheme has advantages and disadvantages, as already discussed in the first part of the paper. It is more important that preserved basin characteristics are adequately described and that well-founded models of depository evolution are given, than choosing a specific classification scheme and basin type therein. With adequate basin-fill description and interpretation, the individual reader can fully understand the nature of the basin and decide for themselves on a specific classification and name, and how well it relates to the basin in question.

Occurrence of basin types over time (and survivability)

For our 25 case study basins, applying the results of the more formal classification schemes as in the preceding section, they can be assigned as foreland basins (n=5), continental rift basins (plume- and non-plume – related; n=7); intracratonic sag basins (n=1); passive margins (n=5); failed rifts (n=5); continental back-arc basins (n=2). These basins range in age from Neoarchaean to Neoproterozoic and they all thus have a significantly long history of preservation. The latter likely relates to the essentially continental character of the basement rocks to each basin and speaks to the "survivability" of these basins. Their preservation over such long time intervals thus relies essentially on the longevity and inherent stability of the continental lithosphere, and thus attests to the survival of these terranes over geological time rather than of the basin-fills themselves. We thus suggest that for sedimentary basins to survive over hundreds to even billions of years of subsequent history, they need to be "cratonized".

This is not to say that basins on and in oceanic lithosphere (e.g., Fig. 5) did not form during the Precambrian past, just that they were seldom preserved, bearing in mind the oldest extensively preserved ocean crust is Jurassic, and that ancient ophiolites (considered by some as controversial) are identified as far back in time as ca. 3.5 Ga (e.g., Chiarenzelli and Moores, 2004). The entire set of arc-related basins (e.g., Fig. 3) almost certainly formed in large numbers within the greenstone belt settings that played such a prominent role in early crustal evolution; however, their deformation and metamorphism often makes effective basin analysis of such preserved depositories challenging (e.g., Eriksson et al., 2013). An example of preserved and identifiable arc-related basins from extensive greenstone deposits is that of the Slave Province in Canada, with the basin-fills dated at ca. 3.1-2.6 Ga (e.g., Corcoran, 2012).

Duration of basins

While the apparent duration of the "cratonized" basins forming the 25 examples discussed here does not differ significantly from the time span of basins discussed earlier in this paper (cf.., Fig. 6), the three Wilson cycles identified for the Kaapvaal craton, the Minas Supergroup (Brazilian shield) and the Huronian Supergroup (Canadian shield) show an interesting temporal relationship, albeit one predicated on a very limited sample of three. The oldest, Kaapvaal, has a Wilson cycle length of ca. ≤398 Myr, that for the next in age, the Minas has acycle length of ca. 540 Myr, and the youngest, the Huronian, a length of ca. 700 Myr. While the entire Wilson cycles themselves appear to get longer over time from these three examples, and while the length of both the rift and the drift phase (the latter including also the ocean shrinking stage), the foreland collisional phase seems to retain a relatively constant length within the overall Wilson cycle duration, of ca. 120 Myr (116 Myr for Kaapvaal, 130 Myr for Minas and 120 Myr for the Huronian). The average duration of Phanerozoic Wilson cycles (ca. 300-400 Myr; Miall, 1997; Fig. 6) appears to have been exceeded by at least some of the Precambrian examples.

PGE acknowledges funding from the University of Pretoria and the National Research Foundation, South Africa. The Geological Society, London is thanked for making this volume possible. Research support to OC was provided by the University of Alberta and the Natural Sciences and Engineering Research Council of Canada. GMY also acknowledges support from the Natural Sciences and Engineering Research Council of Canada. RM is grateful to the University of New South Wales for a post-doctoral fellowship and to Profs. Malcolm Walter and Martin Van Kranendonk for encouragement.

References

ALKMIM, F.F. & MARSHAK, S. 1998. Transamazonian Orogeny in the Southern São Francisco Craton, Minas Gerais, Brazil: Evidence for Paleoproterozoic collision and collapse in the Quadrilátero Ferrífero. *Precambrian Research*, **90**, 29-58

ALKMIM, F.F. & MARTINS-NETO, M.A. 2012. Proterozoic first-order sedimentary sequences of the São Francisco craton, eastern Brazil. *Marine and Petroleum Geology*, **33**, 127-139.

ALKMIM, F.F., MARSHAK, S. & FONSECA, M.A. 2001. Assembling West Gondwana in the Neoproterozoic: Clues from the São Francisco craton region, Brazil. *Geology*, **29**, 319-322.

ALLEN, P.A. & ALLEN, J.R. 2013. *Basin Analysis: Principles and Application to Petroleum Play Assessment*, Third Edition. Wiley-Blackwell, Oxford, 632.

ALMEIDA, F.F.M., BRITO NEVES, B.B. & CARNEIRO, C.D.R. 2000. Origin and evolution of the South American Platform. *Earth-Science Reviews*, **50**, 77-111.

ANDERSON, R.S. 1982. Hotspots, polar wander, Mesozoic convection and the geoid. *Nature*, **297**, 391-393.

ARMSTRONG, R.A., COMPSTON, W., RETIEF, E.A., WILLIAMS, I.S. & WELKE, H.J. 1991. Zircon ion microprobe studies bearing on the age and evolution of the Witwatersrand Triad. *Precambrian Research*, **53**, 243-266.

BABINSKI, M., CHEMALE JR., F. & VAN SCHMUS, W.R. 1995. The Pb/Pb age of the Minas Supergoup carbonate rocks, Quadrilátero Ferrífero, Brazil. *Precambrian Research*, **72**, 235-245.

BAER, A.J. (ed.) 1970. Symposium on Basins and Geosynclines of the Canadian shield. *Geological Survey of Canada Paper*, **70-40**, 265 pp.

BAGAS, L., BIERLEIN, F.P., ENGLISH, L., ANDERSON, J.A.C., MAIDMENT, D. & HUSTON, D.L. 2008.An example of a Palaeoproterozoic back-arc basin: Petrology and geochemistry of the ca. 1864 Ma Stubbins Formation as an aid towards an improved understanding of the Granites-Tanami Orogen, Western Australia. *Precambrian Research*, **166**, 168-184.

BALLY, A.W. 1975. A geodynamic scenario for hydrocarbon occurrences. *Proceedings 9th World Petroleum Congress, Tokyo*, Vol. 2 (Geology), 33-44, Applied Science Publishers, Barking.

BALLY, A.W. & SNELSON, S. 1980. Realms of subsidence. *In*: Miall, A.D. (ed.) *Facts and Principles of World Petroleum Occurrence.* Canadian Society Petroleum Geologists Memoir, **6**, 9-75.

BARBOSA, J.S.F. & SABATÉ, P. 2004. Archean and Paleoproterozoic crust of the São Francisco craton, Bahia, Brazil: geodynamic features. *Precambrian Research*, **133**, 1-27.

BETTS, P.G. 1999. Palaeoproterozoic mid-basin inversion in the northern Mt Isa terrane, Queensland. *Australian Journal of Earth Sciences*, **46**, 735-748.

BETTS, P.G., LISTER, G.S. & POUND, K.S. 1999. Architecture of a Palaeoproterozoic Rift System: Evidence from the Fiery Creek Dome region, Mt Isa terrane. *Australian Journal of Earth Sciences*, **46**, 533-534.

BETTS, P.G., LISTER, G.S. & O'DEA, M.G. 1998.Asymmetric extension of the Middle Proterozoic lithosphere, Mount Isa terrane, Queensland, Australia. *Tectonophysics*, **296**, 293-316.

BETTS, P.G. & GILES, D. 2006. The 1800 Ma to 1100 Ma tectonic evolution of Australia. *Precambrian Research*, **144**, 92-125.

BETTS, P.G., GILES, D., LISTER, G.S. & FRICK, L.R., 2002. Evolution of the Australian Lithosphere. *Australian Journal of Earth Sciences*, **49**, 661-695.

BETTS, P.G., GILES, D. & LISTER, G.S. 2003. Tectonic environment of shale-hosted massive sulphide Pb-Zn-Ag deposits of Proterozoic northeastern Australia. *Economic Geology*, **98**, 557-576.

BETTS, P.G., GILES, D. & AITKEN, A.R.A. 2011. Paleoproterozoic Accretion Processes of Australia and comparisons with Laurentia. *International Geology Reviews*, **53**, 1357-1376.

BETTS, P.G., GILES, D., FODEN, J., SCHAEFER, B.F., MARK, G., PANKHURST, M., FORBES, C.F., WILLIAMS, H.A., CHALMERS, N.C. & HILLS, Q. 2009. Mesoproterozoic plume-modified orogenesis in eastern Precambrian Australia. *Tectonics*, **28(3)**, article 3006, 1-28. doi:10.1029/2008TC002325.

BEUKES, N.J. & CAIRNCROSS, B. 1991. A lithostratigraphic-sedimentological reference profile for the Late Archaean Mozaan Group, Pongola Sequence: application to sequence stratigraphy and correlation with the Witwatersrand Supergroup. *South African Journal of Geology*, **94(1)**, 44-69.

BLEEKER, W. 1994. Taking the pulse of planet Earth: a proposal for a new multi-disciplinary flagship project in Canadian solid earth sciences. *Geoscience Canada,* **31**, 179-190.

BRITO NEVES, B.B. 2011. The Paleoproterozoic in the South-American continent: Diversity in the geologic time. *Journal of South American Earth Sciences*, **32**, 270-286.

BRITO NEVES, B.B., CAMPOS NETO, M.C. & FUCK, R. 1999. From Rodinia to Western Gondwana: An approach to the Brasiliano/Pan-African cycle and orogenic collage. *Episodes*, **22**, 155-199.

BUMBY, A.J., ERIKSSON, P.G., CATUNEANU, O., NELSON, D.R. & RIGBY, M.J. 2012. Meso-Archaean and Palaeo-Proterozoic sedimentary sequence stratigraphy of the Kaapvaal Craton. *Marine and Petroleum Geology*, **33**, 92-116.

BURGESS, P.M., GURNIS, M. & MORESI, L. 1997. Formation of sequences in the cratonic interior of North America by interaction between mantle, eustatic, and stratigraphic processes. *Bulletin Geological Society America,* **108**, 1515-1535.

CAMPBELL, F.H.A. (ed.) 1981. Proterozoic Basins of Canada. *Geological Survey of Canada Paper*, **81-10**, 444 pp.

CAMPBELL, I.H. & ALLEN, C.M. 2008. Formation of supercontinents linked to increases in atmospheric oxygen. *Nature Geoscience,* **1**, 554-558.

CARD, K.D. 1990. A review of the Superior Province of the Canadian Shield, a product of Archean accretion. *Precambrian Research*, **48**, 99-156.

CASTRO, P.T.A. & DARDENNE, M.A. 2000. The sedimentology, stratigraphy and tectonic context of the São Francisco Supergroup at the southern boundary of the São Francisco craton, Brazil. *Revista Brasileira de Geociências*, **30**, 345-437.

CATUNEANU, O. 2001. Flexural partitioning of the Late Archaean Witwatersrand foreland system, South Africa.. *Sedimentary Geology*, **141-142**, 95-112.

CHEMALE, F., DUSSIN, I.A., ALKMIM, F. F., MARTINS, M.S., QUEIROGA, G., ARMSTRONG, R. & SANTOS, M. N. 2012. Unravelling a Proterozoic basin history through detrital zircon geochronology: The case of the Espinhaço Supergroup, Minas Gerais, Brazil. Gondwana Research, **22**, 200-206.

CONDIE, K.C. 2004. Supercontinents and superplume events: distinguishing signals in the geologic record. *Physics of the Earth & Planetary Interiors*, **146**, 319-332.

CONDIE, C.K., O'NEILL, C. & ASTER, R. 2009. Evidence and implications for a widespread magmatic shutdown for 250 My on Earth. *Earth and Planetary Science Letters*, **282**, 294-298.

CONOR, C.H.H. & PREISS, W.V. 2008. Understanding the 1720-1640 Ma Palaeoproterozoic Willyama Supergroup, Curnamona Province, Southeastern Australia: Implications for tectonics, basin evolution and ore genesis. *Precambrian Research*, **166**, 297-317.

CLAOUÉ-LONG, J., MAIDMENT, D. & DONNELLAN, N. 2008. Stratigraphic timing constraints in the Davenport Province, central Australia: A basis for Palaeoproterozoic correlations. *Precambrian Research*, **166**, 204-218.

CLAOUÉ-LONG, J., MAIDMENT, D., HUSSEY, K. & HUSTON, D. 2008.The duration of the Strangways Event in central Australia: Evidence for prolonged deep crust processes. *Precambrian Research*, **166**, 246-262.

CRAMPTON, S.E. & ALLEN, P.A. 1995. Recognition of forebulge unconformities associated with early stage foreland basin development: example from the North Alpine Foreland Basin. *Bulletin American Association of Petroleum Geologists*, **79**, 1495-1514.

DALY, S.J., FANNING, C.M. & FAIRCLOUGH, M.C. 1998. Tectonic evolution and exploration potential of the Gawler Craton. *Australian Geological Survey Organisation Journal of Geology and Geophysics*, **17**, 145-168.

DANDERFER, A., DE WAELE, B., PEDREIRA, A. & NALINI, H.A. 2009. New geochronological constraints on the geological evolution of Espinhaço basin within the São Francisco craton – Brazil. *Precambrian Research*, **170**, 116-128.

DECELLES, P.G. & GILES, K.A. 1996. Foreland basin systems. *Basin Research,* **8**, 105-124.

DE WIT, M.J., ROERING, C., HART, R.J., ARMSTRONG, R.A., DE RONDE, R.E.J., GREEN, R.W.E., TREDOUX, M., PERBERDY, E. & HART, R.A. 1992. Formation of an Archaean continent. *Nature*, **357**, 553-562.

DICKINSON, W.R. 1974. Plate tectonics and sedimentation. *In*: Dickinson, W.R. (ed.) *Tectonics and Sedimentation*. Society of Economic Paleontologists and Mineralogists Special Publication, **22**, 1-27.

DORR, J.V.N. II, 1969. Physiographic, stratigraphic and structural development of the Quadrilátero Ferrífero, Minas Gerais, Brazil. *U.S. Geological Survey Professional Paper*, **641-A**, 1-110.

EINSELE, G. 2000. *Sedimentary Basins: Evolution, Facies and Sediment Budget*, Second Edition. Springer, Berlin, 792.

ELS, B.G. 1998a. The auriferous late Archaean sedimentation systems of South Africa: unique palaeo-environmental conditions? *Sedimentary Geology*, **120**, 205-224.

ELS, B.G. 1998b. The question of alluvial fans in the auriferous Archaean and Proterozoic successions of South Africa. *South African Journal of Geology*, **101/1**, 17-26.

ERIKSSON, K.A., SIMPSON, E.L. & JACKSON M.J. 1993. Stratigraphical evolution of a Proterozoic syn-rift to post-rift basin; constraints on the nature of lithospheric extension in the Mount Isa Inlier, Australia. *In*: Frostick, L.E. & Steel, R.J. (eds.). *Tectonic controls and signatures in sedimentary successions.* International Association of Sedimentologists Special Publication, **20**, 203-221.

ERIKSSON, P.G., ALTERMANN, W. & HARTZER, F.J. 2006. The Transvaal Supergroup and its precursors. *In*: Johnson, M.R., Anhaeusser, C.R. & Thomas, R.J. (eds.). *The Geology of South Africa*. Geological Society of South Africa, Johannesburg and Council for Geoscience, Pretoria, 237-260.

ERIKSSON, P.G., ALTERMANN, W., CATUNEANU, O., VAN DER MERWE, R. & BUMBY, A.J. 2001. Major influences on the evolution of the 2.67-2.1 Ga Transvaal basin, Kaapvaal craton. *Sedimentary Geology*, **141-142**, 205-231.

ERIKSSON, P.G., CONDIE, K.C., VAN DER WESTHUIZEN, W.A., VAN DER MERWE, R., DE BRUIYN, H., NELSON, D.R., ALTERMANN, W. & CUNNINGHAM, M.J. 2002. Late Archaean superplume events: A Kaapvaal-Pilbara perspective. *Journal of Geodynamics*, **34**, 207-247.

ERIKSSON, P.G., BANERJEE, S., NELSON, D.R., RIGBY, M.J., CATUNEANU, O., SARKAR, S., ROBERTS, R.J., RUBAN, D., MTIMKULU, M.N. & SUNDER RAJU, P.V. 2009. A Kaapvaal craton debate: Nucleus of an early small supercontinent or affected by an enhanced accretion event? *Gondwana Research*, **15**, 354-372.

ERIKSSON, P.G., LENHARDT, N., WRIGHT, D.T., MAZUMDER, R. & BUMBY, A.J. 2011. Late Neoarchaean-Palaeoproterozoic supracrustal basin-fills of the Kaapvaal craton: Relevance of the supercontinent cycle, the "Great Oxidation Event" and "Snowball Earth"? *Marine and Petroleum Geology*, **28**, 1385-1401.

FAHRIG, W.F. 1961. The Geology of the Athabasca Formation. *Geological Survey of Canada Bulletin*, **68**, 41 pp.

FISCHER, A.G. 1975. Origin and growth of basins. *In*: Fischer, A.G. & Judson, S. (eds.). *Petroleum and Global Tectonics*. Princeton University Press, Princeton, 47-79.

FORD, M. 2004. Depositional wedge-tops: interaction between low basal friction external orogenic wedges and flexural foreland basins. *Basin Research*, **16**, 361-375.

FRASER, J.A., DONALDSON, J.A., FAHRIG, W.F. & TREMBLAY, L.P. 1970. Helikian basins and geosynclines of the northwestern Canadian shield. *In*: Baer, A.J. (ed.). *Symposium on Basins and Geosynclines of the Canadian shield.* Geological Survey of Canada Paper, **70-40**, 213-238.

FRIMMEL, H.E. 2005. Archaean atmospheric evolution: evidence from the Witwatersrand gold fields, South Africa. *Earth-Science Reviews*, **70**, 1-46.

FUCK, R.A., BRITO NEVES, B.B. & SCHOBBENHAUS, C. 2008. Rodinia descendants in South America. *Precambrian Research*, **160**, 108-126

FURLANETTO, F., THORKELSON, D.J., DANIEL, G.H., MARSHALL, D.D., RAINBIRD, R.H., DAVIS, W.J., CROWLEY, J.L. & VERVOORT, J.D. 2012. Late Paleoproterozoic terrane accretion in northwestern Canada and the case for circum-Columbian orogenesis, *Precambrian Research*, **224**, 512-528. doi:10.1016/j.precamres.2012.10.010

GAO, L.Z., ZHANG, C.H., SHI, X.Y., SONG, B., WANG, Z.Q. & LIU, Y.M.. 2008. Mesoproterozoic age for Xiamaling Formation in North China Plate indicated by zircon SHRIMP dating. *Chinese Science Bulletin*, **53,** 2665–2671.

GIBBS, A.K. & BARRON, C.N. 1993. *The Geology of the Guyana Shield*. Oxford, Clarendon Press, 245.

GIBSON, G. M., RUBENACH, M.J., NEUMANN, N.L., SOUTHGATE, P.N. & HUTTON, L.J. 2008. Syn- and Post-Extensional Tectonic Activity in the Palaeoproterozoic Sequences of Broken Hill and Mount Isa and its Bearing on Reconstructions of Rodinia. *Precambrian Research*, **166**, 350-369.

GILES, D., BETTS, P.G. & LISTER, G.S. 2002. A continental back-arc setting for the Early Proterozoic basins of north-eastern Australia. *Geology*, **30**, 823-826.

GILES, D., BETTS, P.G. & LISTER, G.S. 2004. 1.8-1.5 Ga links between the North and South Australian Cratons and the Palaeo- to Mesoproterozoic configuration of Australia. *Tectonophysics*, **380**, 27-41.

GOULD, S.J. 1989. *Wonderful Life: The Burgess Shale and the Nature of History*. W.W. Norton & Co., New York, 347.

GRIGNÉ, C., LABROSSE, S. & TACKLEY, P.J. 2007. Convection under a lid of finite conductivity: Heat flux scaling and application to continents. *Journal Geophysical Research*, **112**, B08402.

GURNIS, M. 1988. Large-scale mantle convection and the aggregation and dispersal of supercontinents. *Nature*, **332**, 695-699.

HAHN, K., RAINBIRD, R. H. & COUSENS, B. (in press). Sequence stratigraphy, provenance, C and O isotopic composition, and correlation of the Upper Hornby Bay Group and Lower Dismal Lakes Groups, NWT and Nunavut. *Precambrian Research*. doi:10.1016/j.precamres.2012.06.001.

HALBOUTY, M.T., KING, R.E., KLEMME, H.D., DOTT, R.H. & MEYERHOFF, A.A. 1970. World's giant oil and gas fields, geologic factors affecting their formation, and basin classification, part II, Factors affecting formation of giant oil and gas fields, and basin classification. *In:* Halbouty, M.T. (ed.). *Geology of Giant Petroleum Fields*. American Association of Petroleum Geologists Memoir, **14**, 528-555.

HALL, R.C.B. 1996. *The stratigraphic placement of the Venterspost Conglomerate Formation*. MSc thesis, Potchefstroom University for Christian Higher Education, Potchefstroom, South Africa, 153.

HATTON, C.J. 1995. Mantle plume origin for the Bushveld and Ventersdorp magmatic provinces. *Journal of African Earth Sciences*, **21**, 571-577.

HE, Y., ZHAO, G., SUN, M. & XIA, X. 2009. SHRIMP and LA-ICP-MS zircon geochronology of the Xiong'er volcanic rocks: Implications for the Paleo-Mesoproterozoic evolution of the southern margin of the North China Craton. *Precambrian Research*, **168**, 213–222.

HE, Z.J., MENG, X.H., GE, M. & ZHANG, Q. 2000. The early synsedimentary faulting of the Mesoproterozoic Yanshan rift and its influence on event sedimentation. *Journal of Paleogeography*, **2**, 83–91 (in Chinese with English abstract).

HOWARD, K. E., HAND, M., BAROVICH, K. M. & BELOUSOVA, E. 2011. Provenance of late Paleoproterozoic cover sequences in the central Gawler Craton: exploring stratigraphic

correlations in eastern Proterozoic Australia using detrital zircon ages, Hf and Nd isotopic data. *Australian Journal of Earth Sciences*, **58**, 475-500.

HUFF, K.F. 1978. Frontiers of world oil exploration. *Oil and Gas Journal*, **76**, 214-220.

IDNURM, M. & GIDDINGS, J. W. 1995.Paleoproterozoic-Neoproterozoic North America–Australia link: New evidence from paleomagnetism. *Geology*, **23**, 149-152.

INGERSOLL, R.V. 2011. Tectonics of sedimentary basins, with revised nomenclature. *In*: Busby, C.J. & Azor, A. (eds.). *Tectonics of Sedimentary Basins*, Second Edition. Wiley-Blackwell, Oxford, 3-43.

INGERSOLL, R.V. & BUSBY, C.J. 1995. Tectonics of sedimentary basins. *In*: Busby, C.J. & Ingersoll, R.V. (eds.). *Tectonics of Sedimentary Basins.* Blackwell Science, Oxford, 1-52.

JACKSON, M.J., SWEET, I.P. & POWELL, T.G. 1988. Studies on petroleum geology and geochemistry, middle Proterozoic, McArthur Basin, northern Australia; Petroleum potential I. *APEA Journal*, **28**, 283-302.

JACKSON, M.J. & SOUTHGATE, P.N. 2000.Evolution of three unconformity-bounded sandy carbonate successions in the McArthur River region of northern Australia; the Lawn, Wide and Doom supersequences in a proximal part of the Isa Superbasin. *Australian Journal of Earth Sciences*, **47**, 625-635.

KARLSTROM, K.E., ÅHÄLL, K-I., HARLAN, S.S., WILLIAMS, M.L., MCLELLAND, J. & GEISSMAN, J.W. 2001. Long-lived (1.8 - 1.0 Ga) convergent orogen in southern Laurentia, its extensions to Australia and Baltica, and implications for refining Rodinia. *Precambrian Research*, **111**, 5-30.

KERR, R.A. 1985. Plate tectonics goes back 2 billion years. *Science*, **230**, 1364-1367.

KINGSTON, D.R., DISHROON, C.P. & WILLIAMS, P.A. 1983a. Global basin classification. *Bulletin American Association of Petroleum Geology*, **67**, 2175-2193.

KINGSTON, D.R., DISHROON, C.P. & WILLIAMS, P.A. 1983b. Hydrocarbon plays and global basin classification. *Bulletin American Association of Petroleum Geologists*, **67**, 2194-2198.

KINSMAN, D.J.J. 1975. Rift valley basins and sedimentary history of trailing continental margins. *In*: Fischer, A.G. & Judson, S. (eds.). *Petroleum and Global Tectonics.* Princeton University Press, Princeton, 83-126.

KIRKLAND, C.L., SMITHIES, R.H., WOODHOUSE, A.J., HOWARD, H.M.,WINGATE, M.T.D., BELOUSOVA, E.A., CLIFF, J.B., MURPHY, R.C. & SPAGGIARI, C.V. 2013. Constraints and deception in the isotopic record; the crustal evolution of the west Musgrave Province, central Australia. *Gondwana Research*, **23/2**, 759-781.

KLEMME, H.D. 1980. Petroleum basins: classification and characteristics. *Journal Petroleum Geology*, **3**, 187-207.

KORSCH, R.J., HUSTON, D.L., HENDERSON, R.A., BLEWETT, R.S., WITHNALL, I.W., FERGUSSON, C.L., COLLINS, W.J., SAYGIN, E., KOSITCIN, N., MEIXNER, A.J., CHOPPING, R., HENSON, P.A., CHAMPION, D.C., HUTTON, L.J., WORMALD, R., HOLZSCHUH, J. & COSTELLOE, R.D. 2012. Crustal architecture and geodynamics of North Queensland, Australia: Insights from deep seismic reflection profiling. *Tectonophysics*, **572-573**, 76-99.

LAMBECK, A., BAROVICH, K., GIBSON, G., HUSTON, D. & PISAREVSKY, S. 2012. An abrupt change in Nd isotopic composition in Australian basins at 1655Ma: Implications for the tectonic evolution of Australia and its place in NUNA. *Precambrian Research*, **208-211**, 213-221.

LECHEMINANT, A.N. & HEAMAN, L.M. 1989. Mackenzie igneous events, Canada: Middle Proterozoic hotspot magmatism associated with ocean opening. *Earth and Planetary Science Letters*, **96,** 38–48.

LI, H., SU, W., ZHOU, H., GENG, J., XIANG, Z., CUI, Y., LIU, W. & LU, S. 2011. The base age of the Changchengian system at the northern North China craton should be younger than 1670 Ma: constraints from zircon LA-MS-ICPMS dating of a granite-porphyry dike in Miyun county, Beijing. *Earth-Science Frontier*, **18 (3)**, 108–120 (in Chinese with English abstract).

LU, S.N., ZHAO, G.C., WANG, H.M. & HAO, G.J. 2008. Precambrian metamorphic basement and sedimentary cover of the North China Craton: a review. *Precambrian Research*, **160**, 77–93.

MACHADO, N., SCHRANK, A., NOCE, C.M. & GAUTHIER, G. 1996. Ages of detrital zircon from Archean-Paleoproterozoic sequences: Implications for Greenstone Belt setting and evolution of a Transamazonian foreland basin in Quadrilátero Ferrífero, southeast Brazil. *Earth and Planetary Science Letters*, **141**, 259-276

MARTINS-NETO, M.A. 2000. Tectonics and sedimentation in a Paleo/Mesoproterozoic rift-sag basin (Espinhaço basin, southeastern Brazil). *Precambrian Research*, **103**, 147-173.

MARTINS-NETO, M.A., PEDROSA SOARES, A.C. & LIMA, S.A.A. 2001. Tectono-sedimentary evolution of sedimentary basins from Late Paleoproterozoic to Late Neoproterozoic in the São Francisco craton and Araçuaí fold belt, eastern Brazil. *Sedimentary Geology*, **141/142**, 343-370.

MENG, Q.R, WEI, H.H., QU, Y.Q. & MA, S.X. 2011. Stratigraphic and sedimentary records of the rift to drift evolution of the northern North China craton at the Paleo- to Mesoproterozoic transition. *Gondwana Research*, **20**, 205–218.

MIALL, A.D. 2000. *Principles of Sedimentary Basin Analysis*, Third Edition. Springer-Verlag, New York, 616.

NANCE , R.D., WORSLEY, T.R. & MOODY, J.B. 1988. The supercontinent cycle. *Scientific American*, **256**, 72-79.

NAYLOR, M. & SINCLAIR, H. D. 2008. Pro- versus retro-foreland basins. *Basin Research*, **20**, 285-303.

NEUMANN, N.L., SOUTHGATE, P.N., GIBSON, G.M. & MCINTYRE, A. 2006. New SHRIMP geochronology for the Western Fold Belt of the Mt Isa Inlier: Developing a 1800 - 1650 Ma event framework. *Australian Journal of Earth Sciences*, **53**, 1023-1039.

NEUMANN, N.L., SOUTHGATE, P.N. & GIBSON, G.M. 2009. Defining unconformities in Proterozoic sedimentary basins using detrital geochronology and basin analysis - An example from the Mount Isa Inlier, Australia. *Precambrian Research*, **168**, 149-166.

O'DEA, M.G., LISTER, G.S., BETTS, P.G. & POUND, K.S. 1997. A shortened intraplate rift system in the Proterozoic Mount Isa terrane, NW Queensland, Australia. *Tectonics*, **16**, 425-441.

OJAKANGAS, R.W., MOREY, G.B. & GREEN, J.C. 2001. The Mesoproterozoic Midcontinent Rift System, Lake Superior Region, USA. *Sedimentary Geology*, **141–142**, 421–442.

OLSSON, J.R., SÖDERLUND, U., KLAUSEN, M.B. & ERNST, R.E. 2010. U-Pb baddeleyite ages linking major Archean dyke swarms to volcanic rift forming events in the Kaapvaal Craton (South Africa), and a precise age for the BUshveld Complex. *Precambrian Research*, **183**, 490-500.

PAYNE, J.L., BAROVICH, K.M. & HAND, M. 2006. Provenance of metasedimentary rocks in the northern Gawler Craton, Australia: Implications for Palaeoproterozoic reconstructions. *Precambrian Research*, **148**, 275-291.

PAYNE, J.L., HAND M., BAROVICH, K.M., REID, A. & EVANS, D.A.D. 2009. Correlations and Reconstruction Models for the 2500–1500 Ma Evolution of the Mawson Continent. *Geological Society of London Special Publication*, **323**, 319-355.

PEDROSA-SOARES, A.C., NOCE, C.M., WIEDEMANN, C.M. & PINTO, C.P. 2001. The Araçuaí-West Congo orogen in Brazil: An overview of a confined orogen formed during Gondwanland assembly. *Precambrian Research*, **110**, 307-323.

PEDROSA-SOARES, A.C., ALKMIM, F.F., TACK, L., NOCE, C.M., BABINSKI, M., SILVA, L.C. & MARTINS-NETO, M. 2008. Similarities and differences between the Brazilian and African counterparts of the Neoproterozoic Araçuaí-West Congo Orogen. *In*: Pankhurst, J.R., Trouw, R.A.J., Brito Neves, B.B. & De Wit, M.J. (eds.). *West Gondwana: Pre-Cenozoic Correlations across the South Atlantic Region*. Geological Society, London Special Publication, **294**, 153-172.

PENG, P. 2010. Reconstruction and interpretation of giant mafic dyke swarms: a case study of 1.78 Ga magmatism in the North China craton. *In*: Kusky, T. M., Zhai, M.-G. & Xiao, W. (eds.). *The Evolving Continents: Understanding Processes of Continental Growth*. Geological Society, London Special Publication, **338,** 163–178.

PENG, P., ZHAI, M., ZHANG, H. & GUO, J. 2005. Geochronological constraints on the Paleoproterozoic evolution of the North China Craton: SHRIMP zircon ages of different types of mafic dikes. *International Geology Review*, **47**, 492–508.

PIRAJNO, F., HOCKING, R.M., REDDY, S.M. & JONES, A.J. 2009.A review of the geology and geodynamic evolution of the Palaeoproterozoic Earaheedy Basin, Western Australia. *Earth Science Reviews*, **94**, 39-77.

PISAREVSKY, S.A., WINGATE, M.T.D., POWELL, C.M., JOHNSON, S. & EVANS, D.A.D. 2003. Models for Rodinia assembly and fragmentation. *In*: Yoshida, M., Windley, B.F. & Dagupta, S. (eds.). *Proterozoic East Gondwana: Supercontinent Assembly and Breakup*. Geological Society, London Special Publication, **206**, 35-55.

PLANAVSKY, N.J., MCGOLDRICK, P., SCOTT, C.T., LI, C., REINHARD, C.T., KELLY, A.E., CHU, X., BEKKER, A., LOVE, G.D. & LYONS, T.W. 2011.Widespread iron-rich conditions in the mid-Proterozoic ocean. *Nature*, **477**, 448-451.

POTMA, W.A. & BETTS, P.G. 2006. Extension-related structures within the Mitakoodi Culmination: Implications for the nature and timing of extension, and effect on later shortening in the eastern Mount Isa Inlier. *Australian Journal of Earth Sciences*, **53**, 55-67.

PREISS, W.V. 2000. The Adelaide Geosyncline of South Australia and its significance in Neoproterozoic continental reconstruction. *Precambrian Research*, **199**, 21-63.

RAINBIRD, R.H., HEAMAN, L.M. & YOUNG, G.M. 1992. Sampling Laurentia: Detrital zircon geochronology offers evidence for an extensive Neoproterozoic river system originating from Grenville orogen. *Geology*, **20**, 351-354.

RAINBIRD, R.H., & YOUNG, G.M. 2009. Colossal rivers, massive mountains and supercontinents. *Earth,* **54**, 52-61.

RAWLINGS, D.J. 1999. Stratigraphic resolution of a multiphase intracratonic basin system: The McArthur Basin, northern Australia. *Australian Journal of Earth Sciences*, **46**, 703-723.

READING, H.G. (ed.) 1986. *Sedimentary Environments and Facies*, Second Edition. Blackwell, Oxford, 615.

ROBB, L.J. & MEYER, F.M. 1995. The Witwatersrand Basin, South Africa: geological framework and mineralization processes. *Economic Geology Research Unit Information Circular*, University of the Witwatersrand, Johannesburg, **293**, 37pp.

SANTOS, J.O.S. 2003. Geotectonics of the Guyana and Central Brazilian Shields. *In*: Bizzi, L.A., Schobbenhaus, C., Vidotti, R.M. & Gonçalves, J.H. (eds.). *Geology, Tectonics and Mineral Resources of Brazil*. Serviço Geológico – CPRM, Brasília, 169-226

SANTOS, J.O.S., HARTMANN, L.A., GAUDETTE, H.E., GROVES, D.I., MCNAUGHTON, N.J. & FLETCHER, I.R. 2000. A new understanding of the provinces of the Amazon Craton based on integration of field mapping and U-Pb and Sm-Nd geochronology. *Gondwana Research*, **3/4**, 453–488.

SANTOS, J.O.S., POTTER, P.E., REIS, N.J., HARTMANN, L., FLETCHER, I.R. & MCNAUGHTON, N.J. 2003. Age, source, and regional stratigraphy of the Roraima Supergroup and Roraima-like outliers in northern South America based on U-Pb geochronology. *Geological Society of America Bulletin*, **115**, 331-348.

SCHOBBENHAUS, C. & BRITO NEVES, B.B. 2003. Geology of Brazil in the context of the South American Platform. *In*: Bizzi, L.A., Schobbenhaus, C., Vidotti, R.M. & Gonçalves, J.H. (eds.). *Geology, Tectonics and Mineral Resources of Brazil*. Serviço Geológico – CPRM, Brasília, 5-54.

SCOTT, D.L., BRADSHAW, B.E. & TARLOWSKI, C.Z. 1998. The tectonostratigraphic history of the Proterozoic northern Lawn Hill Platform, Australia; an integrated intracontinental basin analysis. *Tectonophysics*, **300**, 329-358.

SCOTT, D.L., RAWLINGS, D.J., PAGE, R.W., TARLOWSKI, C.Z., IDNURM, M., JACKSON, M.J. & SOUTHGATE, P.N. 2000. Basement framework and geodynamic evolution of the Palaeoproterozoic superbasins of north-central Australia: An integrated review of geochemical, geochronological and geophysical data. *Australian Journal of Earth Sciences*, **47**, 341-380.

SCRIMGEOUR, I.R., KINNY, P.D., CLOSE, D.F. & EDGOOSE, C.J. 2005. High-T granulites and polymetamorphism in the southern Arunta Region, central Australia: Evidence for a 1.64 Ga accretion event. *Precambrian Research*, **142**, 1-27.

SHEN, Y., CANFIELD, D.E. & KNOLL, A.H. 2002. Middle Proterozoic ocean chemistry: Evidence from the McArthur Basin, Northern Australia. *American Journal of Science*, **302**, 81-109.

SHEPPARD, S., TYLER, I.M., GRIFFIN, T.J. & TAYLOR, W.R. 1999. Palaeoproterozoic subduction related and passive margin basalts in the Halls Creek Orogen, northwest Australia. *Australian Journal of Earth Sciences*, **46**, 679-690.

SHI, Y., LIU, D., KRÖNER, A.L., JIAN, P., MIAO, L. & ZHANG, F. 2012. Ca. 1318 Ma A-type granite on the northern margin of the North China Craton: Implications for intraplate extension of the Columbia supercontinent. *Lithos*, **148**, 1–9.

SLOSS, L.L. 1963. Sequences in the cratonic interior of North America. *Geological Society of America Bulletin*, **74**, 93-114.

SU, W.B, LI, H.K., HUFF, W.D, ETTENSOHN, F.R., ZHANG, S.H, ZHOU, H.Y. & WAN, Y.S. 2010. SHRIMP U-Pb dating for a K-bentonite bed in the Tieling Formation, North China. *Chinese Science Bulletin*, **55**, 3312–3313.

SOUTHGATE, P.N., BRADSHAW, B.E., DOMAGALA, J., JACKSON, M.J., IDNURM, M., KRASSAY, A.A., PAGE, R.W., SAMI, T.T., SCOTT, D.L., LINDSAY, J.F., MCCONACHIE, B.A. & TARLOWSKI, C.Z. 2000.Chronostratigraphic basin framework for Palaeoproterozoic rocks (1730-1575 Ma) in northern Australia and implications for base-metal mineralisation. *Australian Journal of Earth Sciences*, **47**, 461-483.

SZPUNAR, M., HAND, M., BAROVICH, K., JAGODZINSKI, E. & BELOUSOVA, E. 2011. Isotopic and geochemical constraints on the Paleoproterozoic Hutchison Group, southern Australia:

Implications for Paleoproterozoic continental reconstructions. *Precambrian Research*, **187**, 99-126.

TASSINARI, C.C.G. & MACAMBIRA, M.J.B. 1999. Geochronological provinces of the Amazonian Craton. *Episodes*, **22**, 174–182.

TASSINARY, C.C.G., BETTENCOURT, J.S., GERALDES, M., MACAMBIRA, M. & LAFON, J.M. 2000. The Amazon Craton. *In*: Cordani, U.G., Milani, E.J., Thomaz Fo, A. & Campos, D.A. (eds.). *Tectonic Evolution of South América*. Rio de Janeiro, 31st International Geological Congress, Rio de Janeiro, 41-95.

TEIXEIRA, W., SABATÉ, P., BARBOSA, J., NOCE, C.M. & CARNEIRO, M.A. 2000. Archean and Paleoproterzoic tectonic evolution of the São Francisco craton, Brazil. *In*: Cordani, U.G., Milani, E.J., Thomaz Fo, A. & Campos, D.A. (eds.). *Tectonic Evolution of South América*. Rio de Janeiro, 31st International Geological Congress, Rio de Janeiro, 101-137.

TINKER, J., DE WIT, M.J. & GROTZINGER, J. 2002. Seismic stratigraphic constraints on Neoarchean-Paleoproterozoic evolution of the western margin of the Kaapvaal craton, South Africa. *South African Journal of Geology*, **105**, 107-134.

UHLEIN, A., TROMPETTE, R.R. & EGYDIO-SILVA, M. 1998. Proterozoic rifting and closure, SE border of the São Francisco Craton, Brazil. *Journal of South American Earth Sciences*, **11**, 191-203.

UHLEIN, A., TROMPETTE, R.. & ALVARENGA, C.J.S. 1999. Neoproterozoic glacial and gravitational sedimentation on continental rifted margin: the Jequitaí-Macaúbas sequence (Minas Gerais, Brazil). *Journal of South American Earth Sciences*, **12**, 435-451.

VAN DER WESTHUIZEN, W.A., DE BRUIYN, H. & MEINTJIES, P.G. 1991. The Ventersdorp Supergroup: an overview. *Journal of African Earth Sciences*, **13**, 83-105.

VEEVERS, J.J. 1981. Morphotectonics of rifted continental margins in embryo (East Africa), youth (Africa-Arabia), and maturity (Australia). *Journal of Geology*, **89**, 57-82.

WEIL, A.B., VAN DER VOO, R., NIOCAILL, C.M. & MEERT, J.G. 1998. The Proterozoic supercontinent Rodinia: paleomagnetically derived reconstruction for 1100 to 800 Ma. *Earth and Planetary Science Letters*, **154**, 13-24.

WHITMEYER, S.J. & KARSLTROM, K.E. 2007. Tectonic model for the Proterozoic growth of North America. *Geosphere,* **3**, 220-259.

WILLIAMS, H., HOFFMAN, P.F., LEWRY, J.F., MONGER, J.W.H. & RIVERS, T. 1991**.** Anatomy of North America: thematic geologic portraits of the continent. *Tectonophysics*, **187,** 117-134.

WILSON, T., BOSMAN, S., PHILIP, H., GOUTHAS, G., COWLEY, W., MAUGER, A., BAKER, A., GORDON, G., DHU, T., FAIRCLOUGH, M. & DELANEY, G. 2010. The search for unconformity-related uranium mineralisation in the Pandurra Formation, South Australia: an international multidisciplinary collaboration. *MESA Journal*, **58**, 9-15.

WITHNALL, I.W., BAIN, J.H.C., DRAPER, J.J., MACKENZIE, D.E. & OVERSBY, B.S. 1988. Proterozoic stratigraphy and tectonic history of the Georgetown Inlier, northeastern Queensland. *Precambrian Research*, **40/41**, 429-446.

WOODCOCK, N.H. 2004. Life span and fate of basins. *Geology*, **32**, 685-688. doi:10.1130/G20598.1

WYGRALAK, A.S., AHMAD, M. & HALLENSTEIN, C.P. 1988. Sedimentology of the Westmoreland Conglomerate, southern McArthur Basin, Northern Territory, Australia. *Australian Journal of Earth Sciences*, **35**, 195-207.

YEO, G.M. 1981. The Late Proterozoic Rapitan glaciation in the northern Cordillera. *In*: Baer, A.J. (ed.). *Proterozoic Basins of Canada*. Geological Survey of Canada Paper, **81-10**, 25–46.

YOUNG, G.M. 1978. Proterozoic (<1.7 b.y.) stratigraphy, paleocurrents and orogeny in North America. *Egyptian Journal of Geology,* **22**, 45-64.
YOUNG, G.M., JEFFERSON, C.W., DELANEY, G.D. & YEO, G.M. 1979. Middle and upper Proterozoic evolution of the northern Canadian Cordillera and shield. *Geology*, **7**, 126-128.
YOUNG, G.M., LONG, D.G.F., FEDO, C.M. & NESBITT, H.W. 2001. Paleoproterozoic Huronian basin: product of a Wilson cycle punctuated by glaciations and a meteorite impact. *Sedimentary Geology,* **141-142**, 233-254.
ZEH, A., GERDES, A. & BARTON, J.M., JR. 2009. Archean accretion and crustal evolution of the Kalahari Craton – the zircon age and Hf isotope record of granitic rocks from Barberton/Swaziland to the Francistown Arc. *Journal of Petrology*, **50/5**, 933-966.
ZHANG, S, ZHAO, Y., YANG, Z., HE, Z. & WU, H. 2009. The 1.35 Ga diabase sills from the northern North China Craton: implications for breakup of the Columbia (Nuna) supercontinent. *Earth and Planetary Science Letters*, **288**, 588–600.
ZHANG, S., LIU, S., ZHAO, Y., YANG, J., SONG, B. & LIU, X. 2007. The 1.75–1.68 Ga anorthosite–mangerite–alkali granitoid–rapakivi granite suite from the northern North China Craton: magmatism related to a Paleoproterozoic orogen. *Precambrian Research*, **155**, 287–312.
ZHAO, G.C., SUN, M., WILDE, S.A. & LI, S.Z. 2003. Assembly, accretion and breakup of the Paleo-Mesoproterozoic Columbia Supercontinent: records in the North China Craton. *Gondwana Research*, **6**, 417–434.

Figure captions

Figure 1. Classification schemes from Dickinson (1974) to Kingston *et al.* (1983) emphasizing the plate tectonic setting of the basin.

Figure 2. A simplification of Bally's classification scheme (Bally & Snelson, 1980) based on the concept of the megasuture.

Figure 3. Sedimentary basins in relation to type of lithospheric substrate, location relative to the plate margin, and type of relative plate motion, adapted from Kingston *et al.* 1983, from Allen and Allen (2013, page 16, Fig. 1.15).

Figure 4. Matrix of sedimentary basins in relation to subsidence mechanisms, from Allen & Allen (2013, Fig. 1.16, p. 17) adapted from Ingersoll & Busby (1995). Sedimentary basins are listed according to divergent, convergent, strike-slip kinematics. The main processes acting in these basin types are shown by the shaded cells.

Figure 5. Genetic system for the classification of sedimentary basins based on the primary mechanism for subsidence.

Figure 6. Longevity of basin megasequences and position within the supercontinental 'Wilson' cycle, modified from Woodcock (2004).

Figure 7. Timing of initiation and longevity of a selection of cratonic basins in relation to the two supercontinental cycles of the Phanerozoic. After Allen & Armitage, 2012, Fig. 30.2, p. 605, in Busby & Azor, 2012).

Figure 8. (a) Sketch map of the Kaapvaal craton, showing early southeastern nucleus (made up of Barberton-S and –N terranes), accreted Murchison-North Kaapvaal (MNK) terrane, major Archaean greenstone belts and the Witwatersrand-Pongola, Ventersdorp, Transvaal and Main Waterberg basins. Colesberg magnetic lineament is the suture of the assembled B-S/B-N/MNK terranes with the Kimberley (=westerly accreted terrane) block. The Central Zone (LCZ terrane) of the Limpopo mobile belt subsequently accreted to the north of the assembled Kaapvaal craton. (Modified after de Wit et al. 1992; Tinker et al. 2002; Zeh et al. 2009). (b) Sketch map (top) and schematic profile (line 2-2' on map) through inferred Witwatersrand foreland basin system (below). Preserved Witwatersrand basin equates to foredeep depozone; two solid line half-circles, centred on the areas of maximum loading ("1" and "2" for accreting northern and western composite terranes, respectively), outline the approximate distribution of the foredeep depozone. The forebulge developed outside the area covered by these two half-circles, its apex (point "A") being enclosed by the -130 mgal isoline of the gravity field; three dashed circles suggest contour lines of the foreland system centred around the forebulge apex, with outermost circle marking the back-bulge axis (equates to depo-axis of the Pongola Supergroup basin) (cf. Catuneanu, 2001 and references therein). (c) Schematic basin evolution model for Ventersdorp Supergroup (after Eriksson et al., 2002).

Figure 9. (a) Tectonic map of North America (modified from Whitmeyer and Karlstrom, 2007) to show the location and configuration of the Proterozoic basins discussed in this summary. Note the generally increasing size with time, of orogens and provenance areas that fed siliciclastic materials to big rivers and Proterozoic basins. Extension of Mazatzal-equivalent orogeny on the west side of North America after Furlanetto et al. (2012). (b) Temporal distribution of some North American Proterozoic basins in the context of the supercontinental cycle (after Bleeker, 2004). Multiple glaciations near the beginning and end of the Proterozoic Eon occurred on supercontinents and were preserved in rift basins and on passive margins that developed during continental break-up. Oxygenation of the atmosphere may be associated with these glacial episodes (Campbell and Allen, 2008). Iron formations disappeared for about a billion years (from about 1.7 Ga to – 0.7 Ga).

Figure 10. (a) Tectonic map of South America showing the cratons and Neoproterozoic orogenic systems the Brazilian shield. GS: Guyanas shield; CBS; Central Brazil shield; AS: Atlantic shield. (b) Simplified geologic map of the São Francisco craton and the adjacent Araçuaí orogen showing the distribution of the major Proterozoic lithostratigraphic units, which represent the Minas, Espinhaço, Macaúbas and Bambuí basins.

Figure 11. (a) Geological map of Archaean and Paleoproterozoic geological provinces of Australia with ca 1840-1800 Ma basin distribution superimposed. Approximate location of sections presented in (f-h) is sshown. (b) Geological map of Archaean and Paleoproterozoic geological provinces of Australia with ca 1800-1740 Ma LeichhardtSuperbasin and correlated basins superimposed.(c) Geological map of Archaean and Paleoproterozoic geological provinces of Australia with ca 1725-1680 Ma Calvert Superbasin and correlated basins superimposed. (d)

Geological map of Archaean and Paleoproterozoic geological provinces of Australia with ca 1670-1595 Ma Isa Superbasin and correlated basins superimposed. (e) Simplified Time-Space plot of the basin evolution of Paleoproterzooic Australia. (f) Simplified Tectonic cross section of the Australian Lithosphere during the evolution of the LeichhardtSuperbasin. (g) Simplified Tectonic cross section of the Australian Lithosphere during the evolution of the Calvert Superbasin. (h) Simplified Tectonic cross section of the Australian Lithosphere during the evolution of the Calvert Superbasin. BB: Birrindudu Basin; AI: AruntaInier; DP/TCB: Davenport Province/Tennant Creek Block; EB: Earaheedy Basin; MB: McArthur Basin; MII: Mount Isa Inlier; WMII: Western Mount Isa Inlier; EMII: Eastern Mount Isa Inlier; CP: Curnamona Province; GI: Georgetown Inlier; YP: Yorke Peninsula; YC: YilgarnCraton; PC: Pilbara Craton; TB: Tanami Block; KB: Kimberley Basin; VC: Victoria Basin; CI: Coen Inlier.

Figure 12. Diagram showing Paleo- to Mesoproterozoic stratigraphic and sedimentary sequences (A) and the tectono-sedimentary evolution (B) of the northern North China craton. Note that the NCC basement formed around 1.85 Ga and followed by lithospheric extension, as witnessed by occurrence of widespread mafic dike swarms and A-type granitoid intrusions. Rift basins in the northern North China craton had not initiated until 1650 Ma, and evolved into passive margin since the beginning of the Mesoproterozoic after its dispersal from an adjacent continent. Another phase of crustal extension might have influenced the northern North China craton since the middle Mesoproterozoic.

Table captions

Table 1: Kingston et al.'s (1983) classification scheme as modified by Mitchell & Reading (1986) and Einsele (2000), with synonyms of the main basin types.

Table 2: Basin classification system modified from Ingersoll & Busby (1995) and Ingersoll (2012), following Dickinson (1974, 1976).

Table 1

Basin category	Synonymns
Continental interior sag basins	*Epicontinental basins Intra-cratonic basins*
Continental interior fracture basins	*Grabens, rift valleys Aulacogens*
Passive continental margins	*Margin sags*
Oceanic sag basins	*Nascent ocean basins*
Subduction-related basins	*Deep sea trenches Forearc basins Backarc basins Interarc basins*
Collision-related basins	*Remnant basins Foreland basins (peripheral) Retro-arc basins (intramontane) Broken foreland basins Terrane-related basins (oceanic)*
Strike-slip/wrench basins	*Pull-apart basins (transtensional) Transpressional basins*

Table 2

Basin category	Modern examples	Ancient examples
[1] DIVERGENT SETTINGS		
Continental rifts	*Rio Grande rift; Rhine rift; East African and Ethiopian rifts; Gulf of Corinth, Greece*	*Proterozoic Keeweenawan rift; Triassic Connecticut rift, NE USA; Neogene, Gulf of Suez*
Nascent ocean basins (proto-oceanic troughs) and continental margins	*Red Sea, Gulf of Aden*	*Jurassic, East Greenland*
[2] INTRA-PLATE SETTINGS		
Intra-plate continental margins		
(a) Continental rises and terraces (shelf-slope-rise configuration)	*Eastern Seaboard, USA and Canada*	*Lower Palaeozoic, USA and Canadian Cordillera*
(b) Transform fault configuration	*South coast, west Africa*	*Precambrian-Lower Palaeozoic Alabama-Oklahoma transform*
(c) Embankment configuration (shelf edge above ocean crust)	*Mississippi Gulf Coast*	*Early Palaeozoic Meguma terrane, Canadian Appalachians*
Intracratonic basins	*Chad Basin, Eyre Basin*	*Palaeozoic Michigan and Illinois Basins; Permian-Mesozoic West Siberian Basin*
Continental platforms	*Barents Sea; Eurasian Arctic*	*Lower Palaeozoic Sauk sequence, USA; Russian Platform*
Active ocean basins	*Pacific Ocean basin*	*Semail ophiolite (Oman)*

Oceanic islands, aseismic ridges and plateaus	*Emperor-Hawaii seamount chain*	*Mesozoic Snow Mountain Volcanic Complex (Franciscan), California*
Dormant (no spreading or subduction) ocean basins	*Gulf of Mexico*	*? Palaeozoic Tarim Basin, China*

[3] CONVERGENT SETTINGS

Trenches	*Chile Trench, Japan Trench*	*Cretaceous, Shumagin Island, Alaska; Palaeozoic, Southern Uplands, Scotland*
Trench-slope basins	*Central America Trench*	*Cretaceous Cambria slab, California; Nias Island, Indonesia; Neogene of Hokkaido, Japan*
Fore-arc basins (arc-trench gap)	*Sunda, Indonesia; Alaska Range; Cascades, NW USA-Canada*	*Cretaceous Great Valley sequence, California; Devonian-Carboniferous Tamworth Trough, eastern Australia*
Intra-arc basins	*Median Trough, Nicaraguan Depression*	*Cretaceous Troodos Complex, Cyprus; Oligo-Miocene New hebrides Islands*
Back-arc basins		
(a) oceanic	(*a) Marianas; Sea of Japan; Aleutians back-arc*	*(a) Jurassic Gran Canon Formation, Cedros Island, Baja California*
(b) continental	*(b) Sunda Shelf*	*(b) Upper Triassic-Lower Jurassic USA Cordillera*
Retroforeland basins		
(a) Retro-arc foreland basins	*Sub-Andean basins*	*Cretaceous Sevier foreland, USA; Miocene-Recent Bermejo Basin, Argentina*
(b) Collisional retroforeland basins	*Western Tarim Basin, China*	*Triassic-Jurassic Ordos Basin, China*
(c) Broken retroforeland basins	*Sierras Pampeanas, Argentina*	*Laramide basins, USA (eg. Palaeocene Wind River Basin Wyoming, USA*
Remnant ocean basins (shrinking between convergent margins)	*Bay of Bengal; Huon Gulf (Solomon Sea)*	*Pennsylvanian-Permian, Ouachita Basin, USA; triassic Songpan-Ganzi Zone, central China*
Proforeland basins	*Mesopotamian Basin, Persian Gulf*	*North Alpine Foreland Basin (Swiss Molasse Basin); Indo-Gangetic (sub-Himalayan) Basin*
Wedge-top (piggyback) basins	*Peshawar Basin, Pakistan*	*Neogene Apennines basins, Italy; Cenozoic Tremp-Graus Basin, Spain*

Hinterland basins (on thickened continental crust behind thrust belts)	*Altiplano, Bolivia*	*Neogene Zhada Basin, Tibet*

Basin category	Modern examples	Ancient examples
[4] TRANSFORM SETTINGS		
Transtensional basins (fault-bend basins, stepover basins)	*Dead Sea Basin; Cariaco Basin , offshore Venezuela*	*Carboniferous Magdalen Basin Gulf of St. Lawrence, Canada; Miocene Ridge Basin, California*
Transpressional basins	*Santa Barbara and Ventura basins, southern California*	*Oligo-Miocene San Joaquin Basin, California*
Transrotational basins	*Western Aleutian forearc*	*Miocene Los Angeles Basin, California*
[5] HYBRID & MISCELLANEOUS SETTINGS		
Collisional broken foreland (distant collisions)	*Qaidam Basin, China*	*Pennsylvanian-Permian Taos Trough New Mexico, USA*
Aulacogens (failed rifts at high angle to margin)	*Mississippi Embayment, USA*	*Palaeozoic Anadarko aulacogen Oklahoma, USA; Cretaceous Benue Trough, Nigeria*
Impactogens	*Baikal rift, Siberia*	*Rhine graben, France-Germany*
Successor basins (post-tectonic intermontane basins)	*Southern Basin & Range SW USA*	*Paleogene Sustut Basin, British Columbia, Canada*
Halokinetic basins	*Deep Gulf of Mexico mini-basins*	*Cretaceous-Palaeogene La Popa Basin, Mexico*
Bolide basins	*Meteor Crater, Arizona*	*Cretaceous-Palaeocene boundary Chicxulub Basin (central America)*

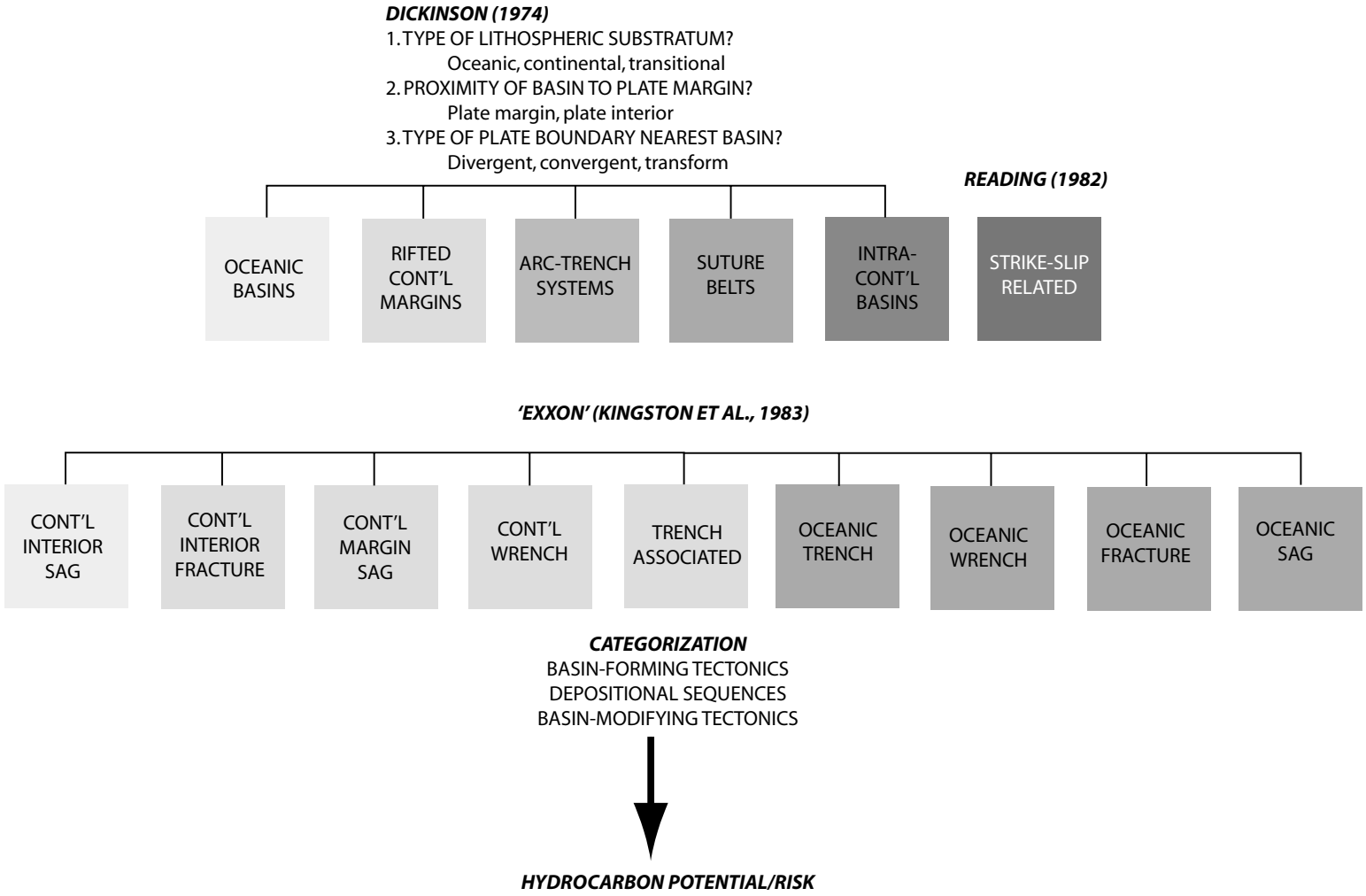
DICKINSON (1974)
1. TYPE OF LITHOSPHERIC SUBSTRATUM?
Oceanic, continental, transitional
2. PROXIMITY OF BASIN TO PLATE MARGIN?
Plate margin, plate interior
3. TYPE OF PLATE BOUNDARY NEAREST BASIN?
Divergent, convergent, transform
READING (1982)
OCEANIC BASINS
RIFTED CONT'L MARGINS
ARC-TRENCH SYSTEMS
SUTURE BELTS
INTRA-CONT'L BASINS
STRIKE-SLIP RELATED
'EXXON' (KINGSTON ET AL., 1983)
CONT'L INTERIOR SAG
CONT'L INTERIOR FRACTURE
CONT'L MARGIN SAG
CONT'L WRENCH
TRENCH ASSOCIATED
OCEANIC TRENCH
OCEANIC WRENCH
OCEANIC FRACTURE
OCEANIC SAG
CATEGORIZATION
BASIN-FORMING TECTONICS
DEPOSITIONAL SEQUENCES
BASIN-MODIFYING TECTONICS
HYDROCARBON POTENTIAL/RISK

Figure 1

1 RIGID, STABLE LITHOSPHERE

1.1 Related to ocean crust formation
1.1.2 Rifts; *1.1.2* Oceanic transform fault associated; *1.1.3* Oceanic abysssal plains;
1.1.4 Atlantic-type passive margins straddling oceanic and continental crust
1.2 Located on pre-Mesozoic continental lithosphere
1.2.1 Cratonic basins

2 RIGID LITHOSPHERE OUTSIDE CONTRACTIONAL MEGASUTURES: *'PERISUTURAL'*

2.1 Deep sea trench on oceanic crust associated with Benioff-type subduction
2.2 Foredeep on continental crust adjacent to Amferer-type subduction
2.2.1 Ramp with buried grabens but no block-faulting; *2.2.2* Dominated by block-faulting
2.3 Chinese-type basins associated with no subduction

3 WITHIN MEGASUTURES: *'EPISUTURAL'*

3.1 Associated with Benioff-type subduction
3.1.1 Forearc basins; *3.1.2* Circum-Pacific backarc basins on oceanic crust (marginal sea) or continental crust
3.2 Backarc basins associated with continental collision
3.2.1 *Pannonian-type* basins on continental crust; *3.2.2 Western Mediterranean-type* basins on transitional or oceanic crust
3.3 Related to episutural megashear systems
3.3.1 *Great Basin-type* basins; 3.3.2 *California-type* basins

Figure 2

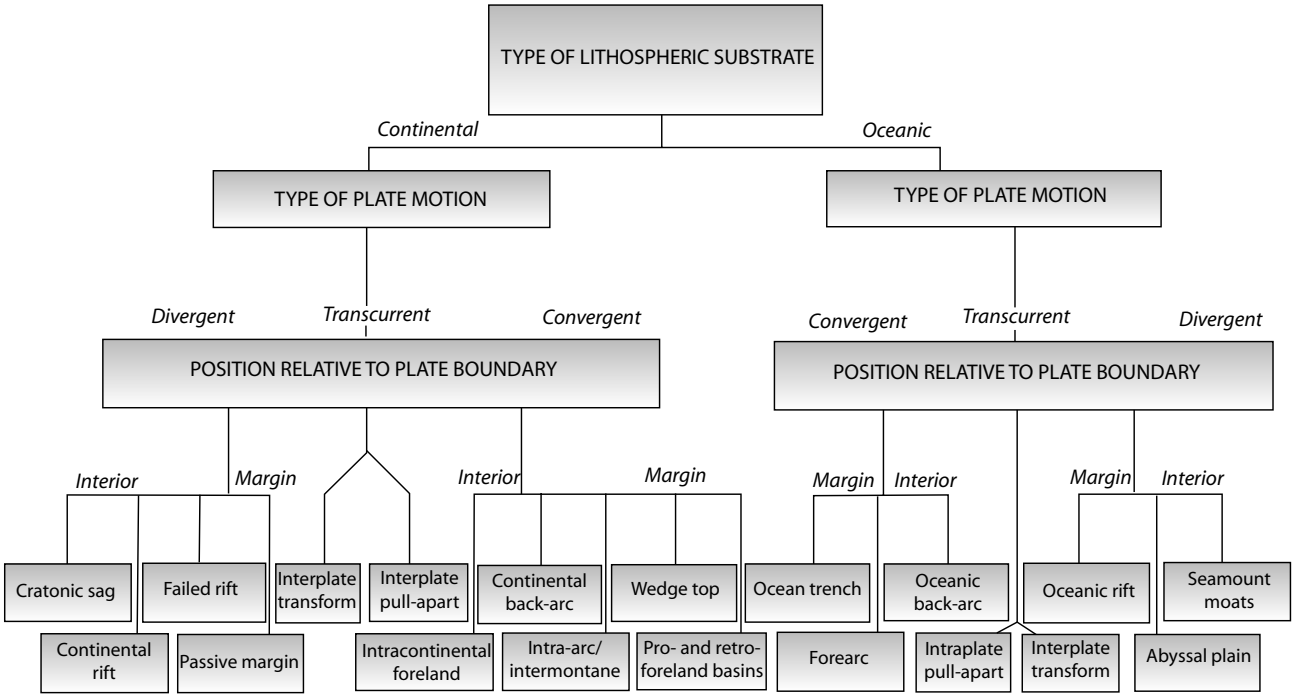
TYPE OF LITHOSPHERIC SUBSTRATE
Continental
Oceanic
TYPE OF PLATE MOTION
TYPE OF PLATE MOTION
Divergent
Transcurrent
Convergent
Convergent
Transcurrent
Divergent
POSITION RELATIVE TO PLATE BOUNDARY
POSITION RELATIVE TO PLATE BOUNDARY
Interior
Margin
Interior
Margin
Margin
Interior
Margin
Interior
Cratonic sag
Failed rift
Interplate transform
Interplate pull-apart
Continental back-arc
Wedge top
Ocean trench
Oceanic back-arc
Oceanic rift
Seamount moats
Continental rift
Passive margin
Intracontinental foreland
Intra-arc/ intermontane
Pro- and retro-foreland basins
Forearc
Intraplate pull-apart
Interplate transform
Abyssal plain

Figure 3

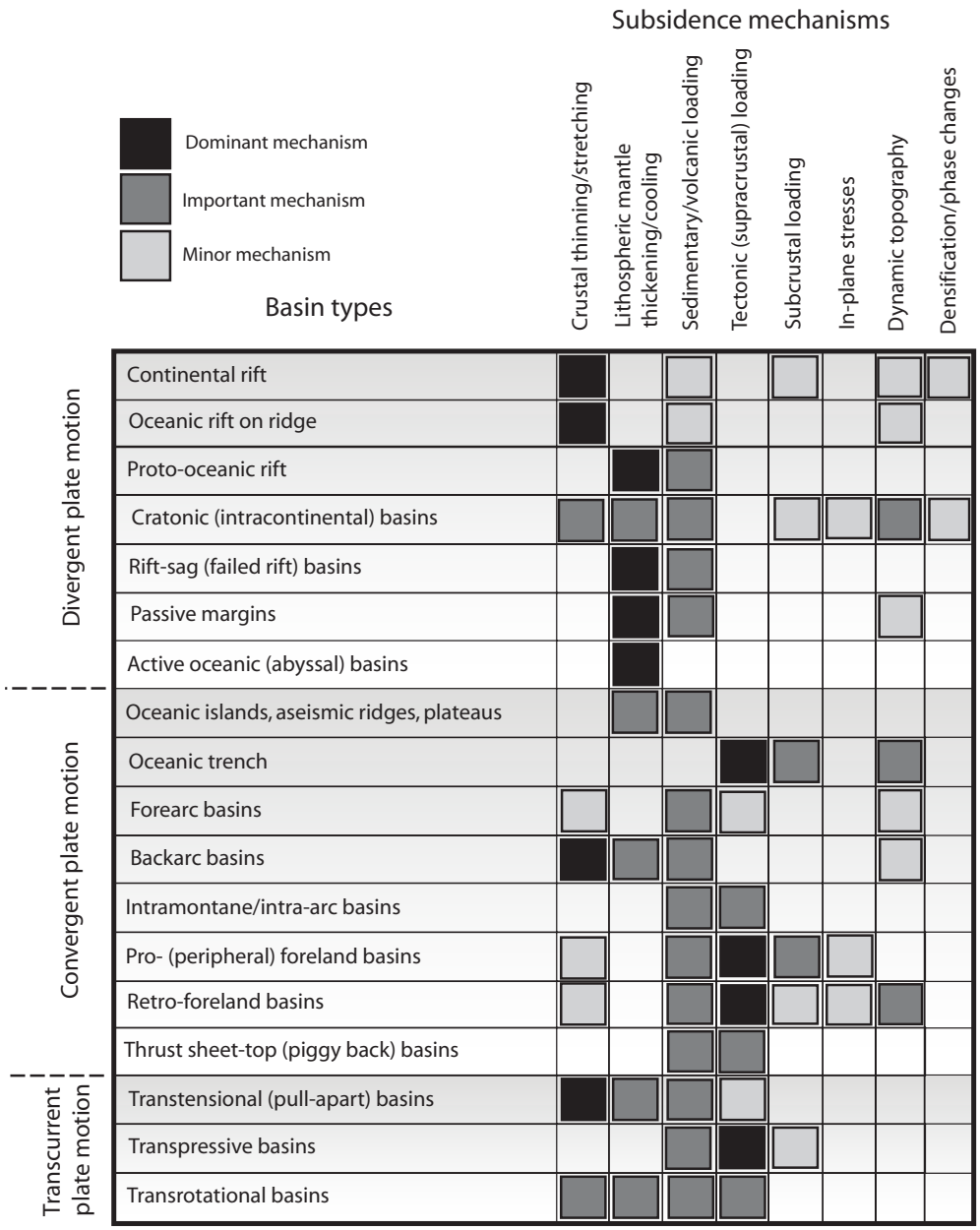
Subsidence mechanisms
Dominant mechanism
Important mechanism
Minor mechanism
Basin types
Crustal thinning/stretching
Lithospheric mantle thickening/cooling
Sedimentary/volcanic loading
Tectonic (supracrustal) loading
Subcrustal loading
In-plane stresses
Dynamic topography
Densification/phase changes
Divergent plate motion
Convergent plate motion
Transcurrent plate motion
Continental rift
Oceanic rift on ridge
Proto-oceanic rift
Cratonic (intracontinental) basins
Rift-sag (failed rift) basins
Passive margins
Active oceanic (abyssal) basins
Oceanic islands, aseismic ridges, plateaus
Oceanic trench
Forearc basins
Backarc basins
Intramontane/intra-arc basins
Pro- (peripheral) foreland basins
Retro-foreland basins
Thrust sheet-top (piggy back) basins
Transtensional (pull-apart) basins
Transpressive basins
Transrotational basins

Figure 4

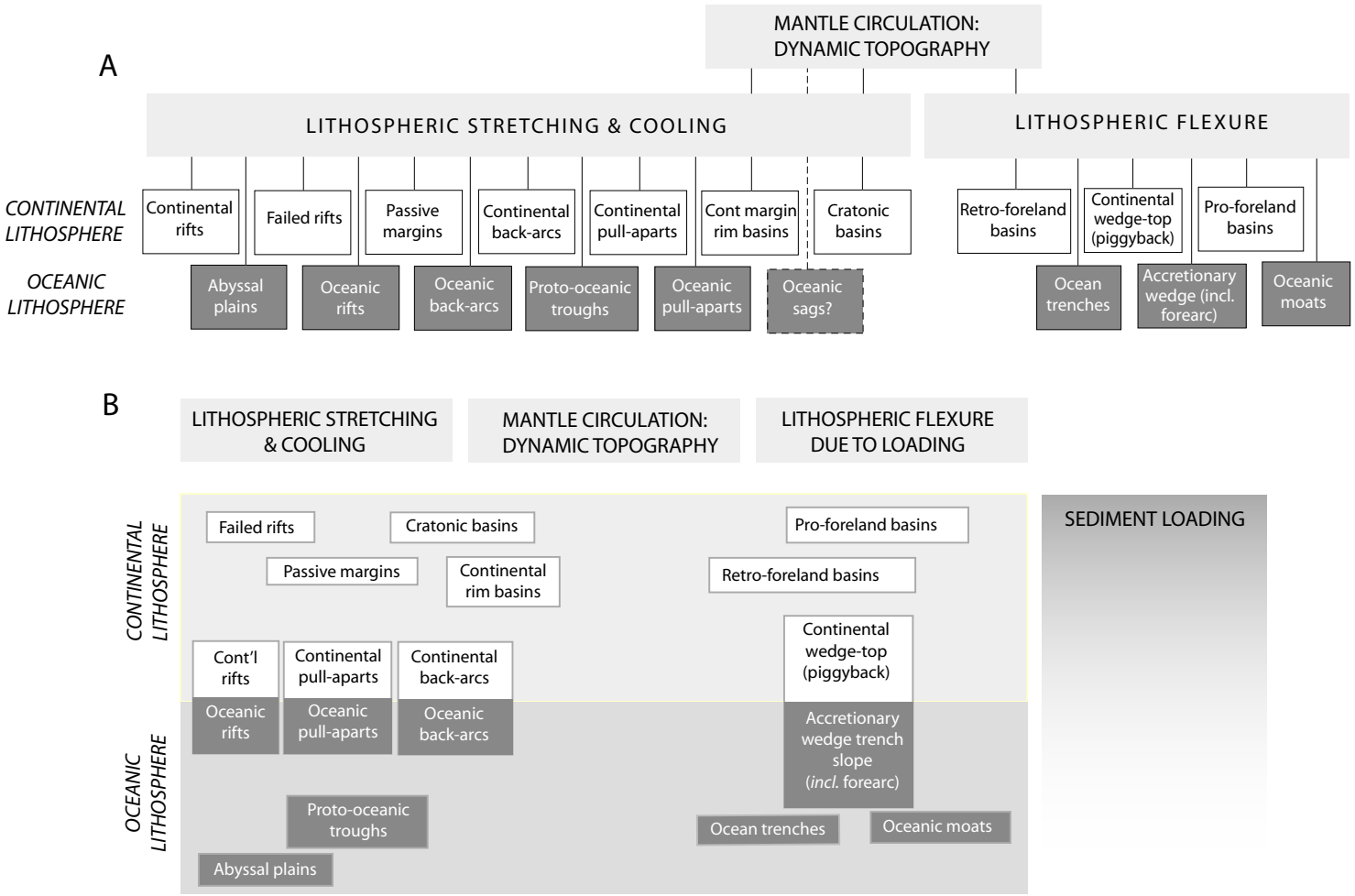
A
MANTLE CIRCULATION: DYNAMIC TOPOGRAPHY
LITHOSPHERIC STRETCHING & COOLING
LITHOSPHERIC FLEXURE
CONTINENTAL LITHOSPHERE
OCEANIC LITHOSPHERE
Continental rifts
Failed rifts
Passive margins
Continental back-arcs
Continental pull-aparts
Cont margin rim basins
Cratonic basins
Retro-foreland basins
Continental wedge-top (piggyback)
Pro-foreland basins
Abyssal plains
Oceanic rifts
Oceanic back-arcs
Proto-oceanic troughs
Oceanic pull-aparts
Oceanic sags?
Ocean trenches
Accretionary wedge (incl. forearc)
Oceanic moats
B
LITHOSPHERIC STRETCHING & COOLING
MANTLE CIRCULATION: DYNAMIC TOPOGRAPHY
LITHOSPHERIC FLEXURE DUE TO LOADING
SEDIMENT LOADING
CONTINENTAL LITHOSPHERE
OCEANIC LITHOSPHERE
Failed rifts
Cratonic basins
Passive margins
Continental rim basins
Pro-foreland basins
Retro-foreland basins
Continental wedge-top (piggyback)
Cont'l rifts
Continental pull-aparts
Continental back-arcs
Oceanic rifts
Oceanic pull-aparts
Oceanic back-arcs
Accretionary wedge trench slope (incl. forearc)
Proto-oceanic troughs
Ocean trenches
Oceanic moats
Abyssal plains

Figure 5

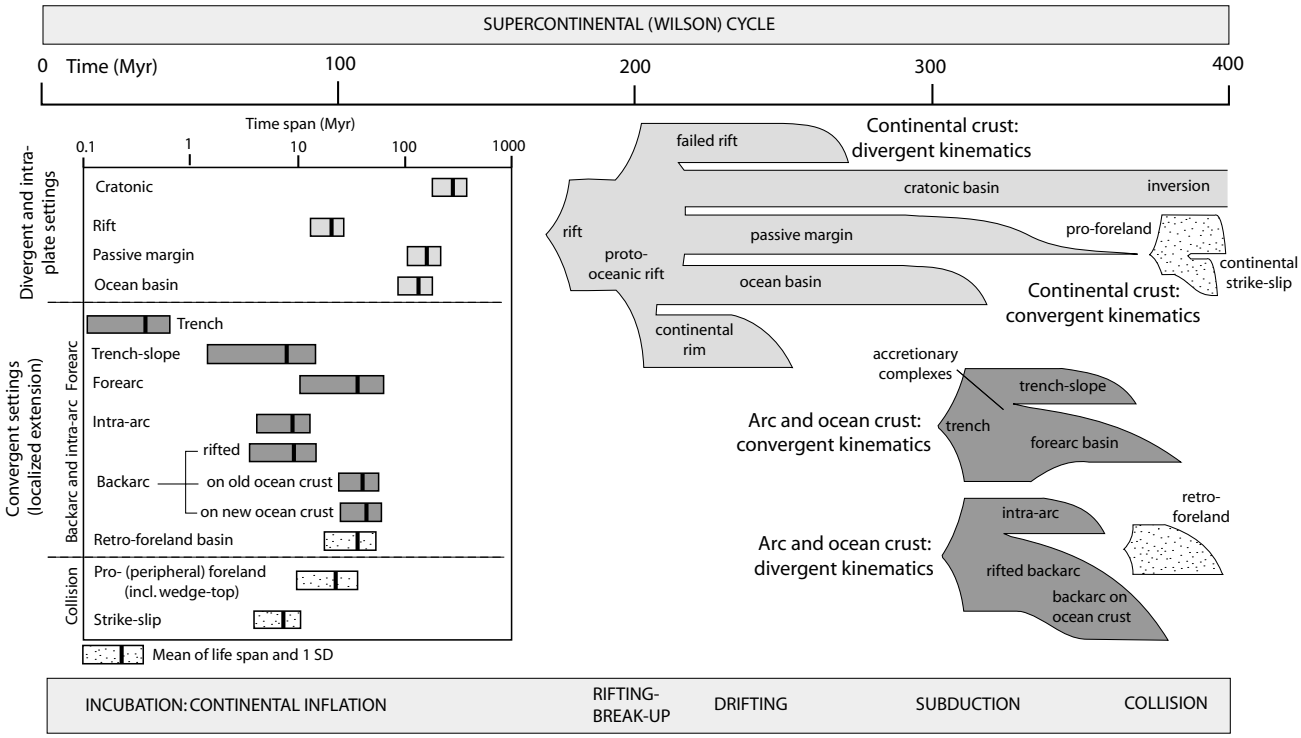
SUPERCONTINENTAL (WILSON) CYCLE
0
Time (Myr)
100
200
300
400
Time span (Myr)
0.1
1
10
100
1000
Divergent and intra-plate settings
Cratonic
Rift
Passive margin
Ocean basin
Convergent settings (localized extension)
Forearc
Trench
Trench-slope
Forearc
Backarc and intra-arc
Intra-arc
Backarc
rifted
on old ocean crust
on new ocean crust
Retro-foreland basin
Collision
Pro- (peripheral) foreland (incl. wedge-top)
Strike-slip
Mean of life span and 1 SD
failed rift
Continental crust: divergent kinematics
cratonic basin
inversion
rift
passive margin
pro-foreland
proto-oceanic rift
continental strike-slip
ocean basin
Continental crust: convergent kinematics
continental rim
accretionary complexes
trench-slope
Arc and ocean crust: convergent kinematics
trench
forearc basin
retro-foreland
intra-arc
Arc and ocean crust: divergent kinematics
rifted backarc
backarc on ocean crust
INCUBATION: CONTINENTAL INFLATION
RIFTING-BREAK-UP
DRIFTING
SUBDUCTION
COLLISION

Figure 6

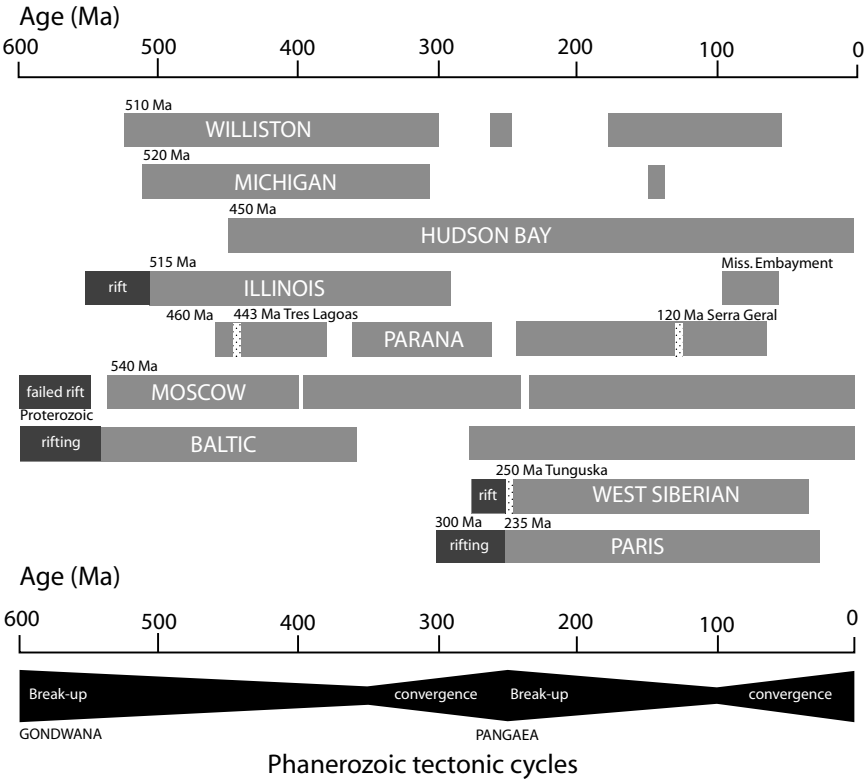

Phanerozoic tectonic cycles

Figure 7

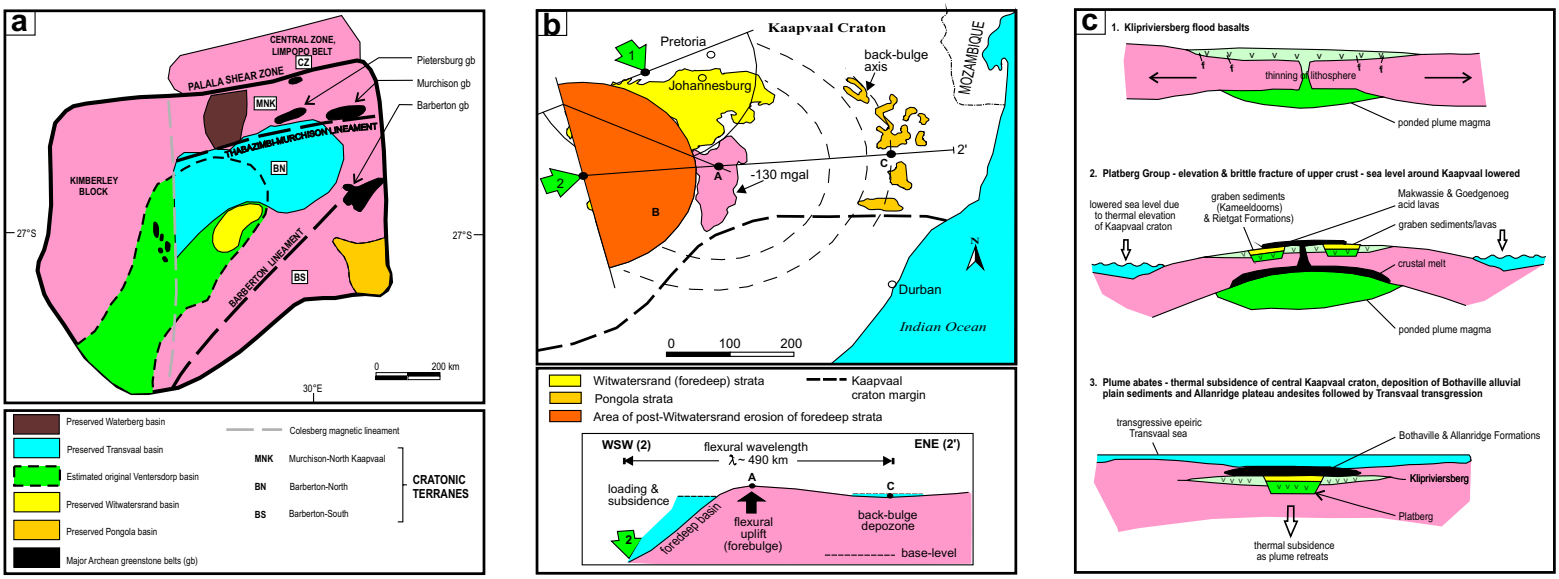
a
CENTRAL ZONE, LIMPOPO BELT
CZ
PALALA SHEAR ZONE
MNK
Pietersburg gb
Murchison gb
Barberton gb
THABAZIMBI-MURCHISON LINEAMENT
BN
KIMBERLEY BLOCK
BARBERTON LINEAMENT
BS
27°S
27°S
0
200 km
30°E
Preserved Waterberg basin
Preserved Transvaal basin
Estimated original Ventersdorp basin
Preserved Witwatersrand basin
Preserved Pongola basin
Major Archean greenstone belts (gb)
Colesberg magnetic lineament
MNK Murchison-North Kaapvaal
BN Barberton-North
BS Barberton-South
CRATONIC TERRANES
b
Kaapvaal Craton
Pretoria
Johannesburg
back-bulge axis
MOZAMBIQUE
1
2
2'
A
C
-130 mgal
B
Durban
Indian Ocean
0
100
200
Witwatersrand (foredeep) strata
Pongola strata
Area of post-Witwatersrand erosion of foredeep strata
Kaapvaal craton margin
WSW (2)
flexural wavelength
λ ~ 490 km
ENE (2')
loading & subsidence
foredeep basin
flexural uplift (forebulge)
back-bulge depozone
base-level
c
1. Klipriviersberg flood basalts
thinning of lithosphere
ponded plume magma
2. Platberg Group - elevation & brittle fracture of upper crust - sea level around Kaapvaal lowered
lowered sea level due to thermal elevation of Kaapvaal craton
graben sediments (Kameeldooms) & Rietgat Formations)
Makwassie & Goedgenoeg acid lavas
graben sediments/lavas
crustal melt
ponded plume magma
3. Plume abates - thermal subsidence of central Kaapvaal craton, deposition of Bothaville alluvial plain sediments and Allanridge plateau andesites followed by Transvaal transgression
transgressive epeiric Transvaal sea
Bothaville & Allanridge Formations
Klipriviersberg
Platberg
thermal subsidence as plume retreats

Figure 8

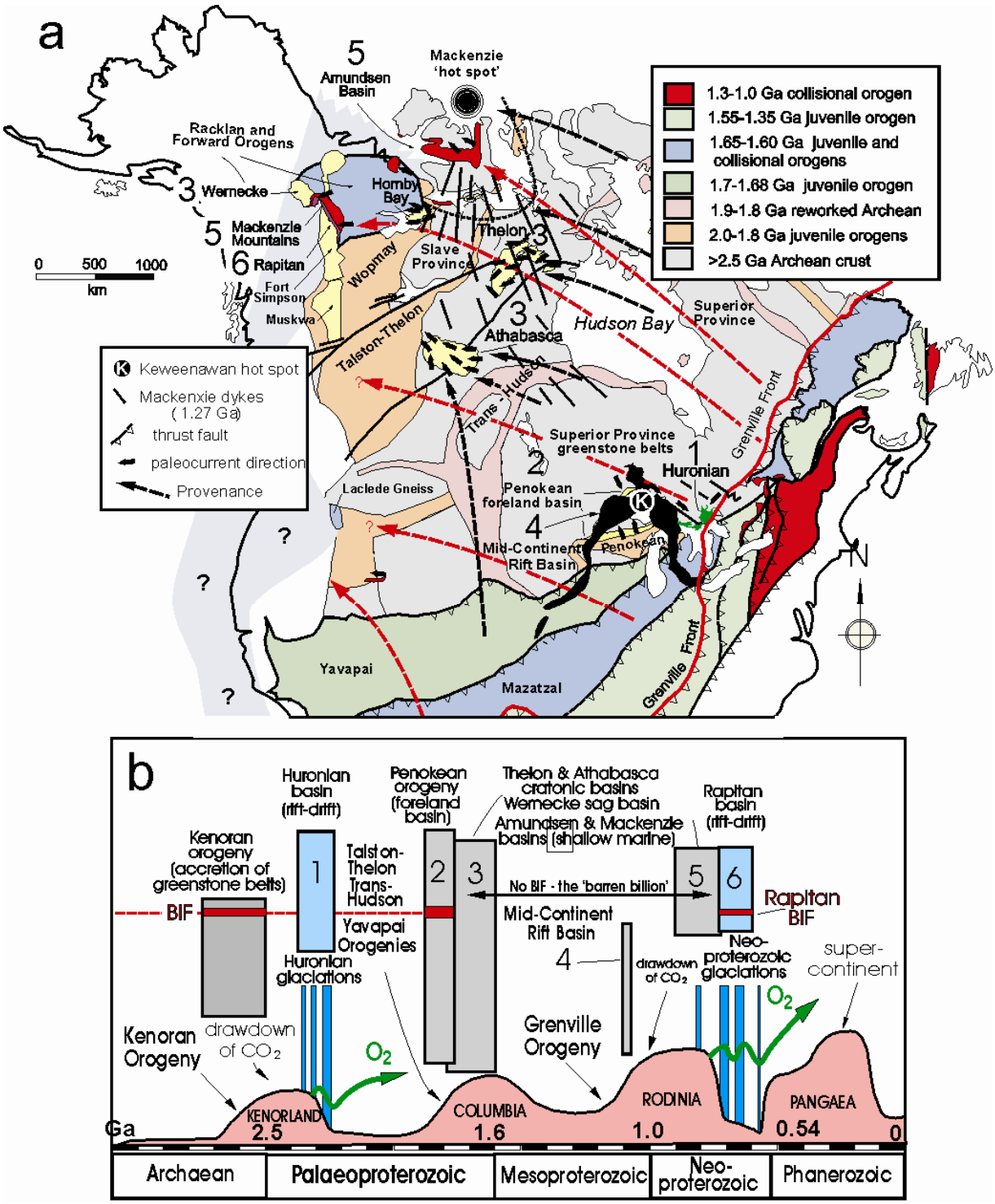
a
5
Amundsen Basin
Mackenzie 'hot spot'
Racklan and Forward Orogens
3 Wernecke
Hornby Bay
5 Mackenzie Mountains
6 Rapitan
Fort Simpson
Muskwa
Wopmay
Slave Province
Thelon
3
Athabasca
Hudson Bay
Superior Province
Talston-Thelon
Trans-Hudson
Grenville Front
Superior Province greenstone belts
2
1
Huronian
Laclede Gneiss
Penokean foreland basin
4
Mid-Continent Rift Basin
Penokean
Yavapai
Mazatzal
Grenville Front
N
0 500 1000
km
1.3-1.0 Ga collisional orogen
1.55-1.35 Ga juvenile orogen
1.65-1.60 Ga juvenile and collisional orogens
1.7-1.68 Ga juvenile orogen
1.9-1.8 Ga reworked Archean
2.0-1.8 Ga juvenile orogens
>2.5 Ga Archean crust
K Keweenawan hot spot
Mackenxie dykes (1.27 Ga)
thrust fault
paleocurrent direction
Provenance
b
Huronian basin (rift-drift)
Penokean orogeny (foreland basin)
Thelon & Athabasca cratonic basins
Wernecke sag basin
Amundsen & Mackenzie basins (shallow marine)
Rapitan basin (rift-drift)
Kenoran orogeny (accretion of greenstone belts)
1
Talston-Thelon
Trans-Hudson
2
3
No BIF - the 'barren billion'
5
6
BIF
Rapitan BIF
Yavapai Orogenies
Mid-Continent Rift Basin
4
Huronian glaciations
drawdown of CO_2
Neo-proterozoic glaciations
super-continent
Kenoran Orogeny
drawdown of CO_2
O_2
Grenville Orogeny
O_2
KENORLAND
2.5
COLUMBIA
1.6
RODINIA
1.0
PANGAEA
0.54
0
Ga
Archaean
Palaeoproterozoic
Mesoproterozoic
Neo-proterozoic
Phanerozoic

Figure 9

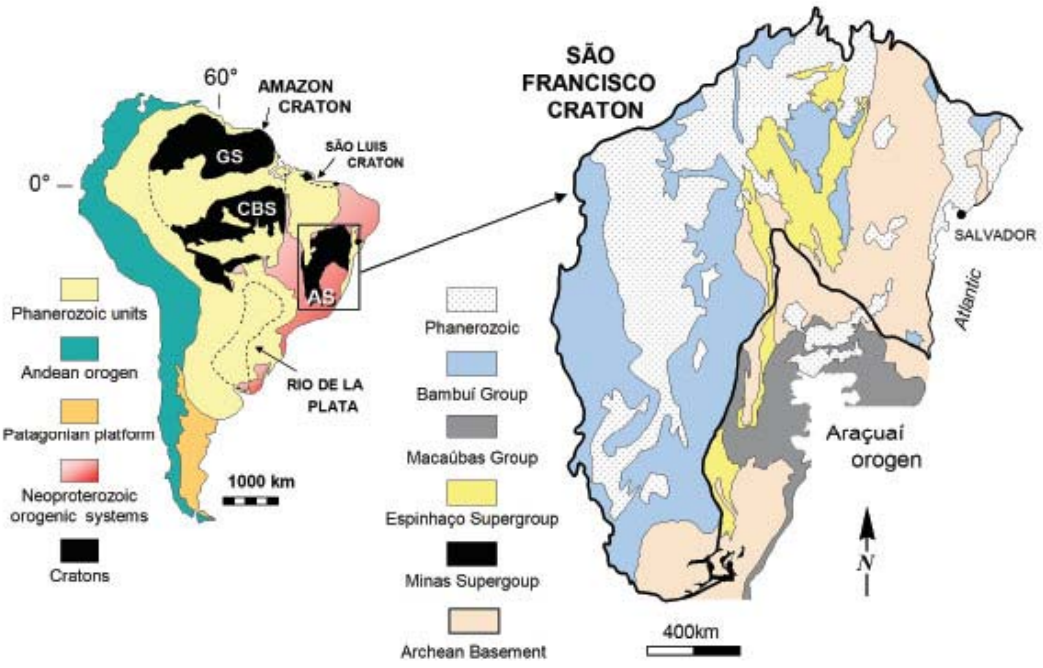
60°
0°
AMAZON CRATON
SÃO LUIS CRATON
GS
CBS
AS
RIO DE LA PLATA
1000 km
Phanerozoic units
Andean orogen
Patagonian platform
Neoproterozoic orogenic systems
Cratons
SÃO FRANCISCO CRATON
SALVADOR
Atlantic
Araçuaí orogen
N
400km
Phanerozoic
Bambuí Group
Macaúbas Group
Espinhaço Supergroup
Minas Supergoup
Archean Basement

Figure 10

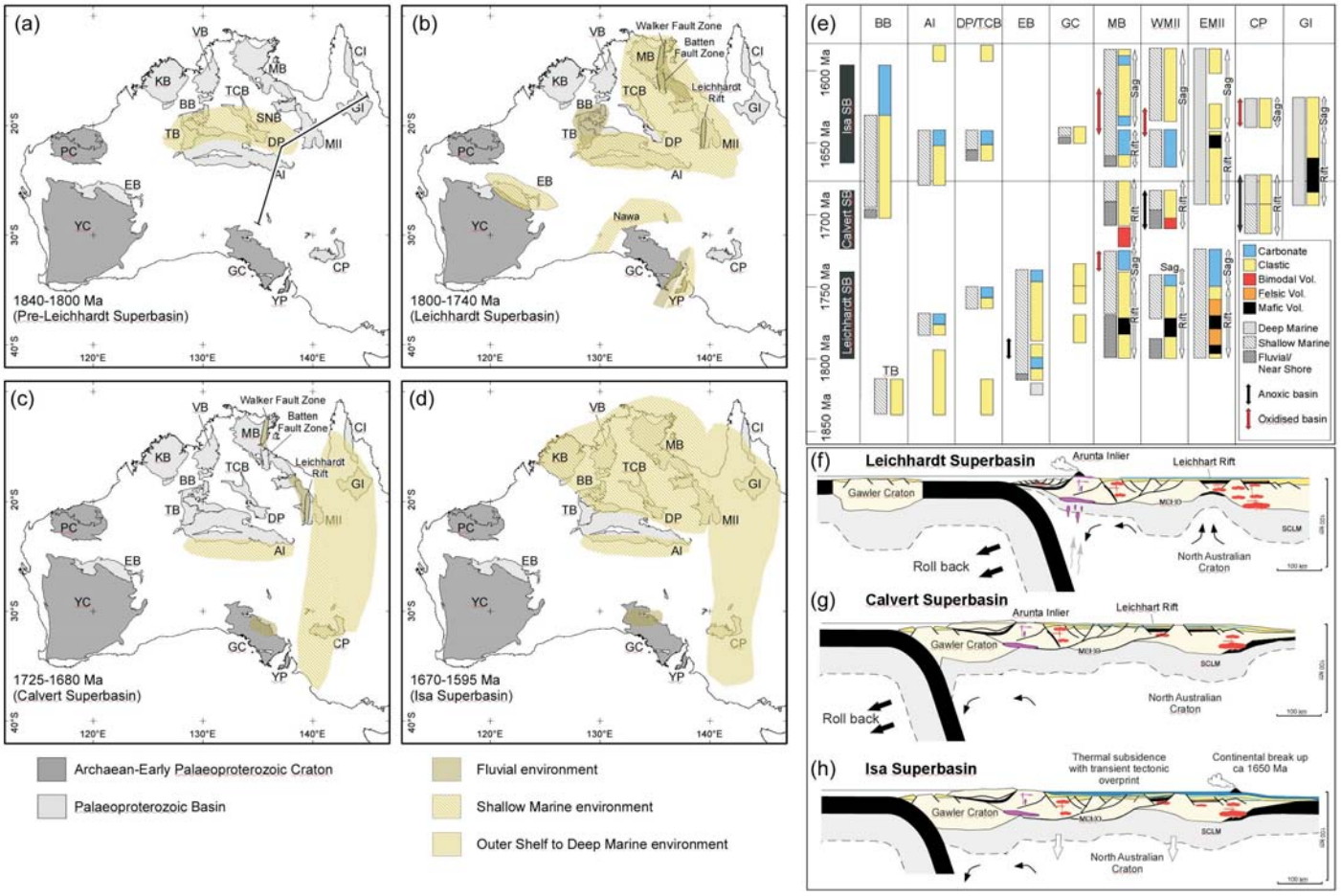
(a)
1840-1800 Ma
(Pre-Leichhardt Superbasin)
(b)
1800-1740 Ma
(Leichhardt Superbasin)
(c)
1725-1680 Ma
(Calvert Superbasin)
(d)
1670-1595 Ma
(Isa Superbasin)
VB
KB
TCB
BB
SNB
TB
DP
MII
AI
PC
EB
YC
GC
YP
CP
GI
CI
MB
Walker Fault Zone
Batten Fault Zone
Leichhardt Rift
Nawa
20°S
30°S
40°S
120°E
130°E
140°E
Archaean-Early Palaeoproterozoic Craton
Palaeoproterozoic Basin
Fluvial environment
Shallow Marine environment
Outer Shelf to Deep Marine environment
(e)
BB
AI
DP/TCB
EB
GC
MB
WMII
EMII
CP
GI
1600 Ma
1650 Ma
1700 Ma
1750 Ma
1800 Ma
1850 Ma
Isa SB
Calvert SB
Leichhardt SB
Sag
Rift
Carbonate
Clastic
Bimodal Vol.
Felsic Vol.
Mafic Vol.
Deep Marine
Shallow Marine
Fluvial/
Near Shore
Anoxic basin
Oxidised basin
(f)
Leichhardt Superbasin
Arunta Inlier
Leichhart Rift
Gawler Craton
Roll back
North Australian
Craton
MCLD
SCLM
(g)
Calvert Superbasin
(h)
Isa Superbasin
Thermal subsidence
with transient tectonic
overprint
Continental break up
ca 1650 Ma

Figure 11

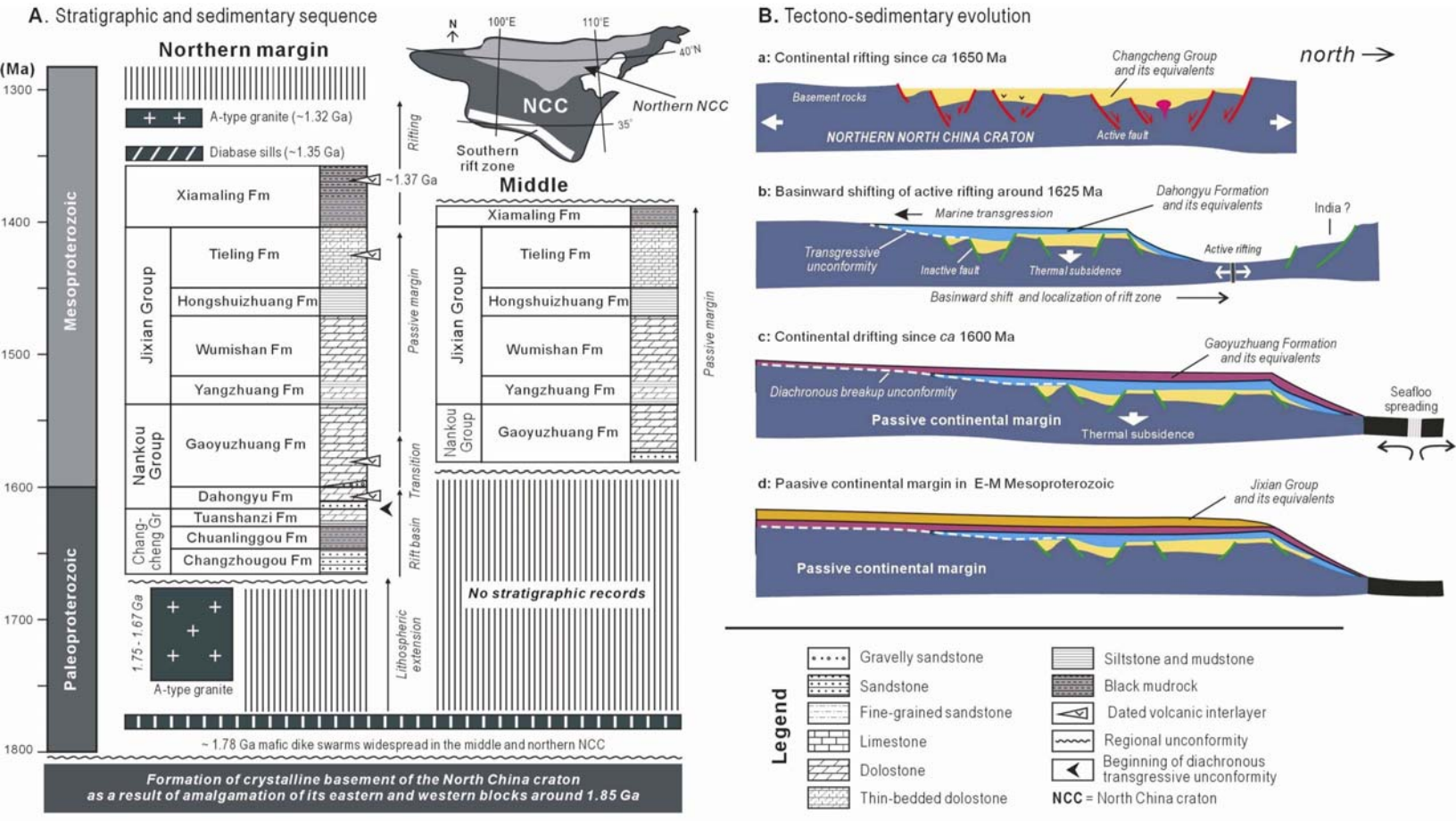
A. Stratigraphic and sedimentary sequence
Northern margin
Middle
(Ma)
1300
1400
1500
1600
1700
1800
Mesoproterozoic
Paleoproterozoic
A-type granite (~1.32 Ga)
Diabase sills (~1.35 Ga)
~1.37 Ga
Xiamaling Fm
Jixian Group
Tieling Fm
Hongshuizhuang Fm
Wumishan Fm
Yangzhuang Fm
Nankou Group
Gaoyuzhuang Fm
Dahongyu Fm
Chang-cheng Gr
Tuanshanzi Fm
Chuanlinggou Fm
Changzhougou Fm
1.75 - 1.67 Ga
A-type granite
Rifting
Passive margin
Transition
Rift basin
Lithospheric extension
No stratigraphic records
~ 1.78 Ga mafic dike swarms widespread in the middle and northern NCC
Formation of crystalline basement of the North China craton
as a result of amalgamation of its eastern and western blocks around 1.85 Ga
N
100°E
110°E
40°N
35°
NCC
Northern NCC
Southern rift zone
B. Tectono-sedimentary evolution
a: Continental rifting since ca 1650 Ma
Changcheng Group and its equivalents
north
Basement rocks
NORTHERN NORTH CHINA CRATON
Active fault
b: Basinward shifting of active rifting around 1625 Ma
Dahongyu Formation and its equivalents
Marine transgression
India ?
Transgressive unconformity
Inactive fault
Thermal subsidence
Active rifting
Basinward shift and localization of rift zone
c: Continental drifting since ca 1600 Ma
Gaoyuzhuang Formation and its equivalents
Diachronous breakup unconformity
Passive continental margin
Thermal subsidence
Seafloo spreading
d: Paasive continental margin in E-M Mesoproterozoic
Jixian Group and its equivalents
Passive continental margin
Legend
Gravelly sandstone
Sandstone
Fine-grained sandstone
Limestone
Dolostone
Thin-bedded dolostone
Siltstone and mudstone
Black mudrock
Dated volcanic interlayer
Regional unconformity
Beginning of diachronous transgressive unconformity
NCC = North China craton

Figure 12